

# Process Analytical Technology and the Question of Scale

International Society for Lyophilization – Freeze Drying  
7th International Conference  
Barcelona, Spain  
6 July - 10 July, 2015

# Overview

- Highlight from the CDER PAT guidance document (2004)
- Brief overview of scale lengths
- Features and limitations of existing PAT
- Through Vial Impedance Spectroscopy (TVIS): Overview
- TVIS Applications & Challenges
  - Ice formation
  - Phase behaviour ( $T_{EU}$  and  $T_G$ )
  - Annealing & structural relaxation
  - Various scales (freeze-drier heterogeneity, ice front shape)
- TVIS Future developments

# Process Analytical Technology

The desired state of pharmaceutical manufacturing and regulation may be characterized as follows:

- Product quality and performance are ensured through the design of **effective and efficient** manufacturing processes
- Product and process specifications are based on a **mechanistic understanding** of how formulation and process factors affect product performance
- ..... Etc

This defines the role for PAT in the concurrent development of the product and process (and not just for manufacturing controls)

## **Guidance for Industry PAT — A Framework for Innovative Pharmaceutical Development, Manufacturing, and Quality Assurance**

U.S. Department of Health and Human Services  
Food and Drug Administration  
Center for Drug Evaluation and Research (CDER)  
Center for Veterinary Medicine (CVM)  
Office of Regulatory Affairs (ORA)

Pharmaceutical CGMPs  
September 2004



## Scale of Scrutiny

### Nano

(0.1 – 100 nm)

Molecules,  
macromolecules,  
nano-particles  
**CQA** : drug stability

### Meso 1

(1 nm – 1  $\mu$ m)

short range order/fractality  
co-operativity (CRR) & dynamics,  
microviscosity, phase separation

**CPP** :  $T_G$ ,  $T_C$

### Macro-bulk

(cm to m)

Vials (individual  
& clusters)  
engineering scales  
**CPP**:  
Temperature &  
drying rate distributions

### “Meso 2”

(100  $\mu$ m to cm?)

Pore connectivity  
**CPP**:  
dry layer resistance

### Micro-bulk

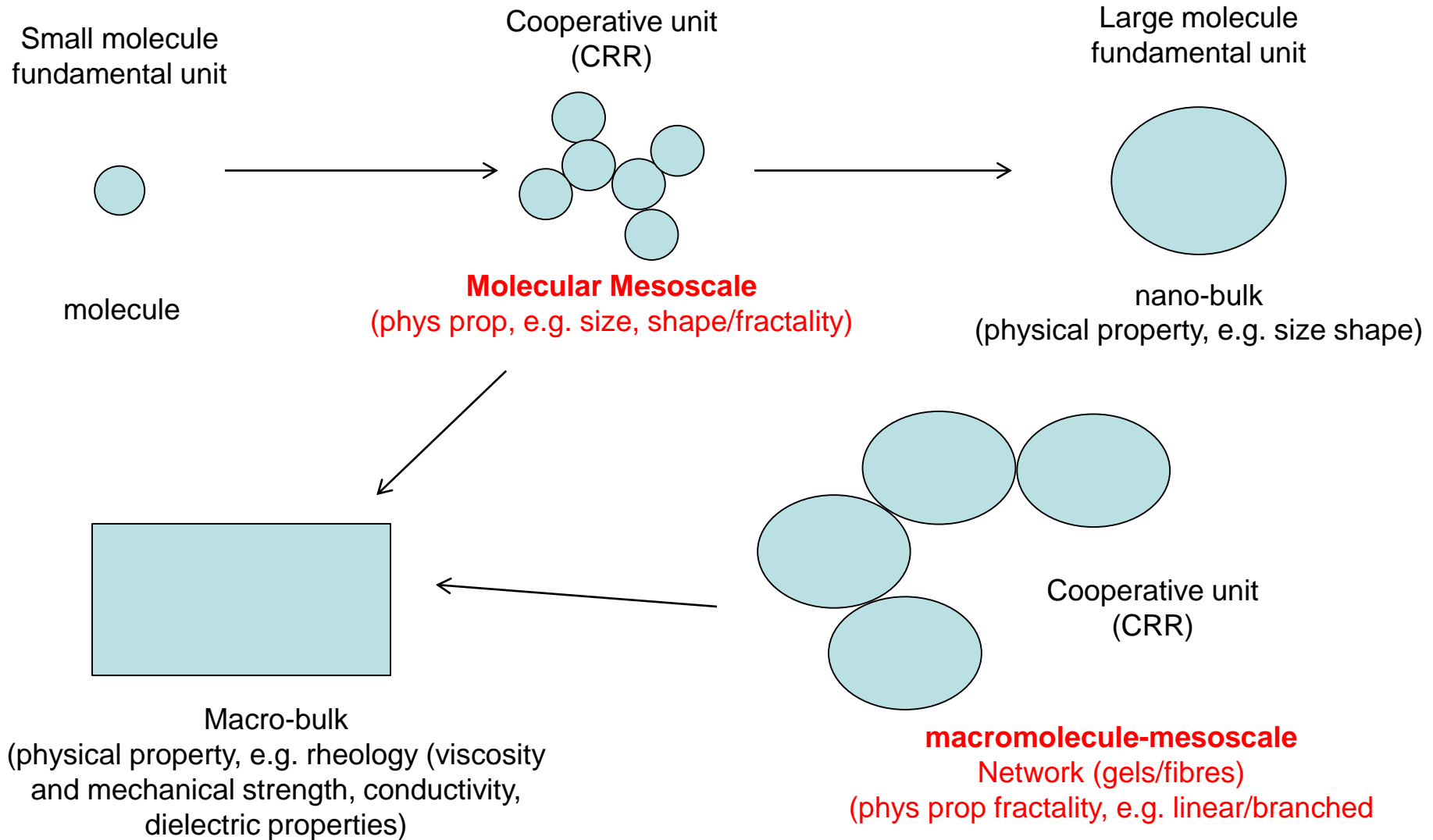
(1 – 50  $\mu$ m)

- crystal size/shape distributions
- crystal habit
- enthalpy of fusion

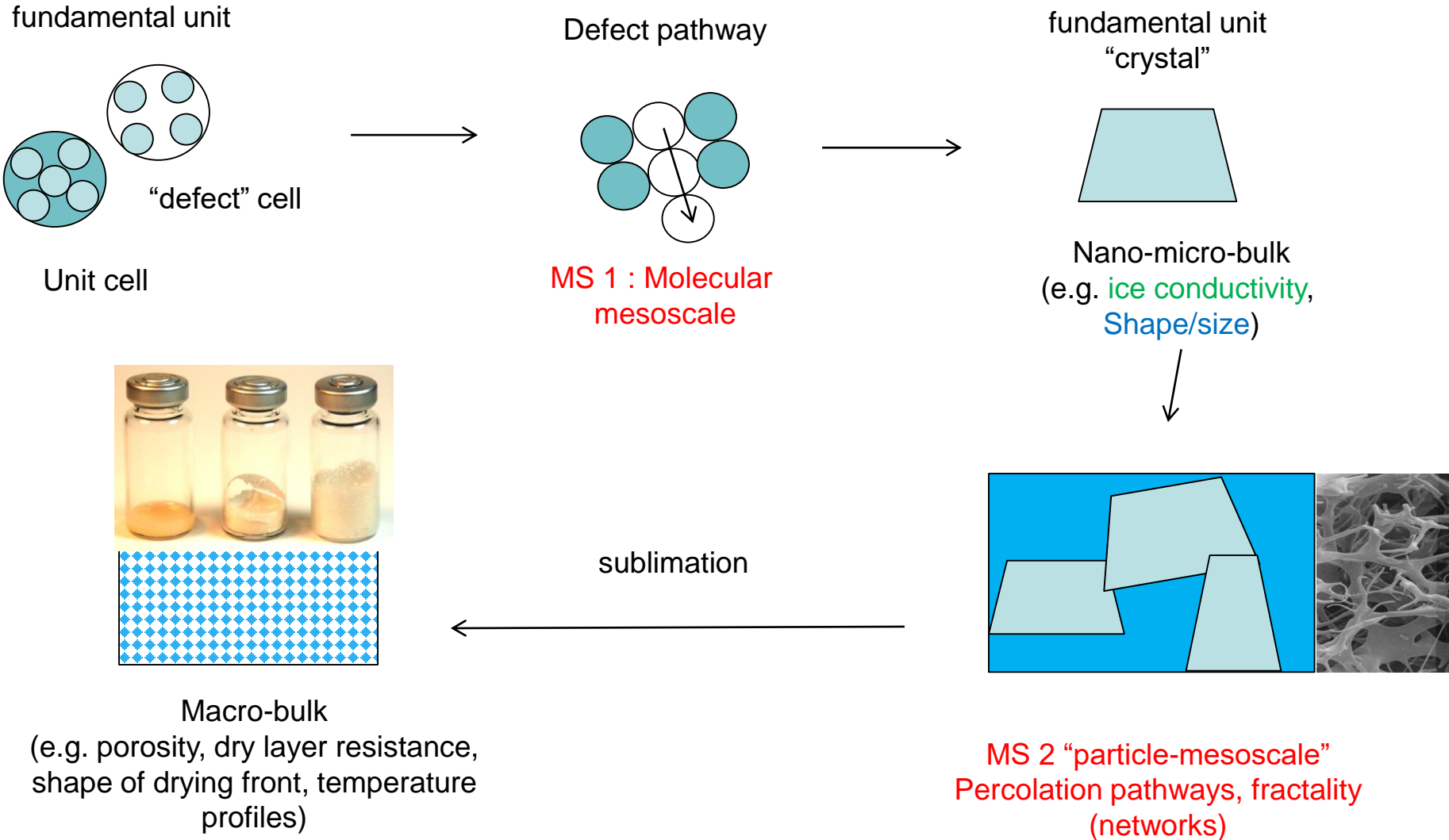
**CPP** :  $T_{EU}$



# Mesoscale in amorphous systems



# Mesoscales in crystalline materials



# PAT and scale length

- PAT can be in-line or off-line (e.g. of the later : DSC and FDM)
- The classic distinction is to divide in-line PAT methods into those applicable to **single vials** and those that measure **the batch**

## Single vial techniques are for localised measurements

- **Thermal Information** TC & RTD provide pin point measurements of temperature (more suited to small scale R&D if wired sensors, wireless can be used at larger scale)
  - multiple sensors are required to monitor distributions of temperature within an individual vial or across populations of vials
- **Molecular Information** Spectroscopic techniques measure through the glass and may not access the core of a vial (penetration depth depends on absorption coefficient of the contents)
  - Many are difficult to locate within a batch process and are best used for novel continuous processes, whereby the vials can be transported through a sensing region and the ice layer is reduced to 1-2 mm

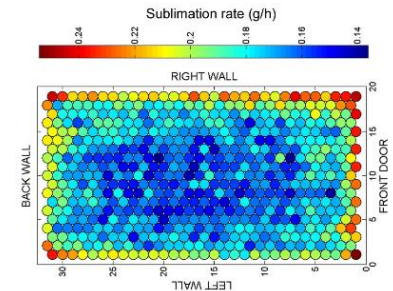


# PAT and scale length

- The classic distinction is to divide PAT methods into those applicable to **single vials** and those that measure **the batch**

## Batch techniques provide an average measurement

- Good for end point determination in primary drying
- Some cant be used at small scale (TDLAS) so not useful in mini-pilot studies
- In order to ensure that they are representative – need to address the heterogeneity in the thermal behaviour of the system (e.g. through pressure drop, ice fog nucleation and controlled crystal growth)

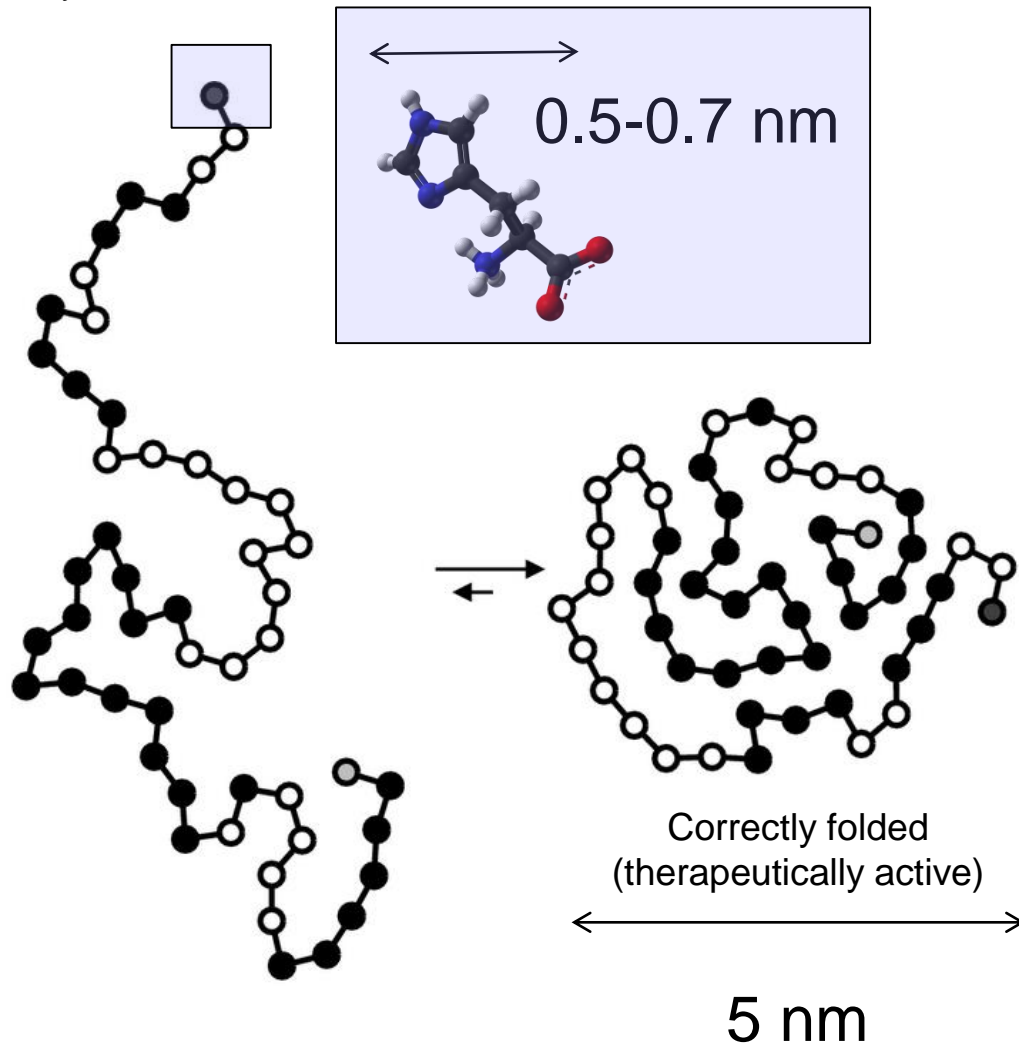


- Given the **essential nature of the batch process** it is difficult to imagine a single PAT method that can translate across all scales.



"L-histidine-zwitterion-  
from-xtal-1993-3D-balls-  
B" by Ben Mills

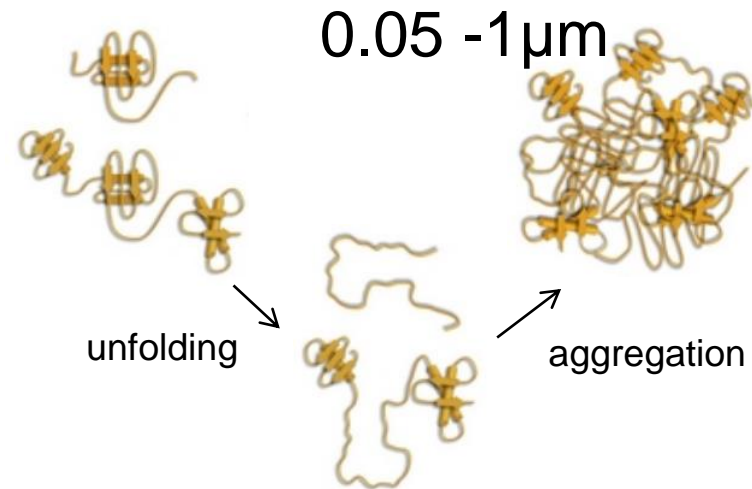
## Nano (1 – 1000 nm)



### Molecular scale inc size/shape

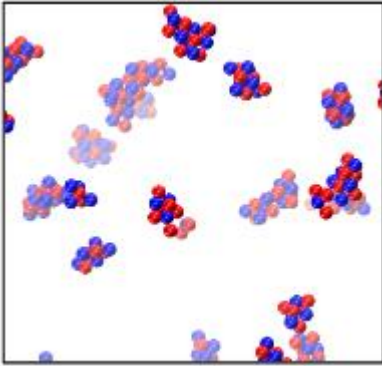
#### CQA : Product stability

unfolding and/or Incorrect  
protein folding can inactivate  
a therapeutic protein and  
may lead to irreversible  
aggregation (& possible  
immunogenicity)

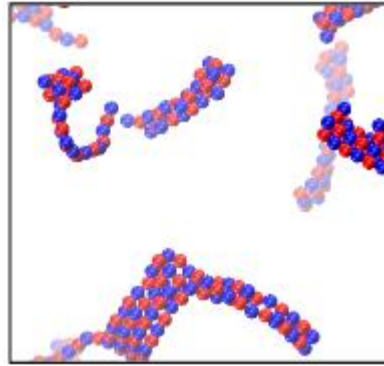


# Meso scale (<1 nm – 100 μm?)

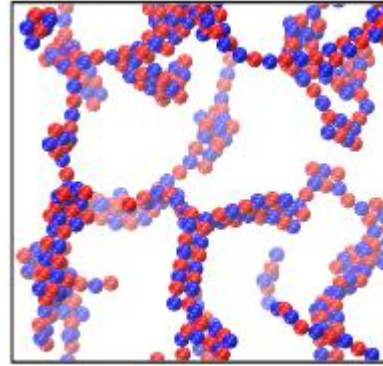
- An intermediate scale (between scales) often associated with clusters of fundamental units



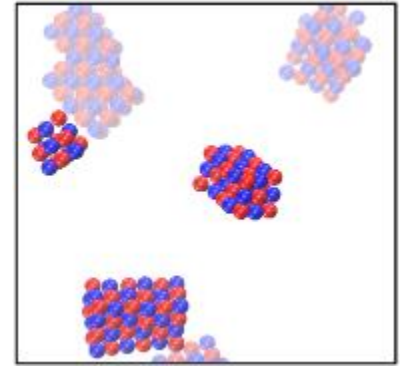
Disordered cluster/CRR



fibrils



networks



crystalline cluster

- Scale length depends on the numbers, the assembly pattern and the size of the fundamental unit, e.g. small molecule, large molecule, or nano-particle
- The assembly pattern can define the short range order and may be characterised by fractality, defects, **molecular dynamics & cooperativity**
- **CQA : Product stability**, e.g. protein aggregation impacts product efficacy and safety

# TVIS

- A more recent addition to the suit of available PAT is the use of impedance measurements across a vial rather than within the vial (as in the CHRIST system)
- Hence the term **Through Vial Impedance Spectroscopy**
- Impedance is a frequency dependent parameter largely because both the impedance of a capacitance or an inductor are both dependent on the frequency of the applied field.
- By fitting the impedance spectrum one can extract the sample resistance and capacitance

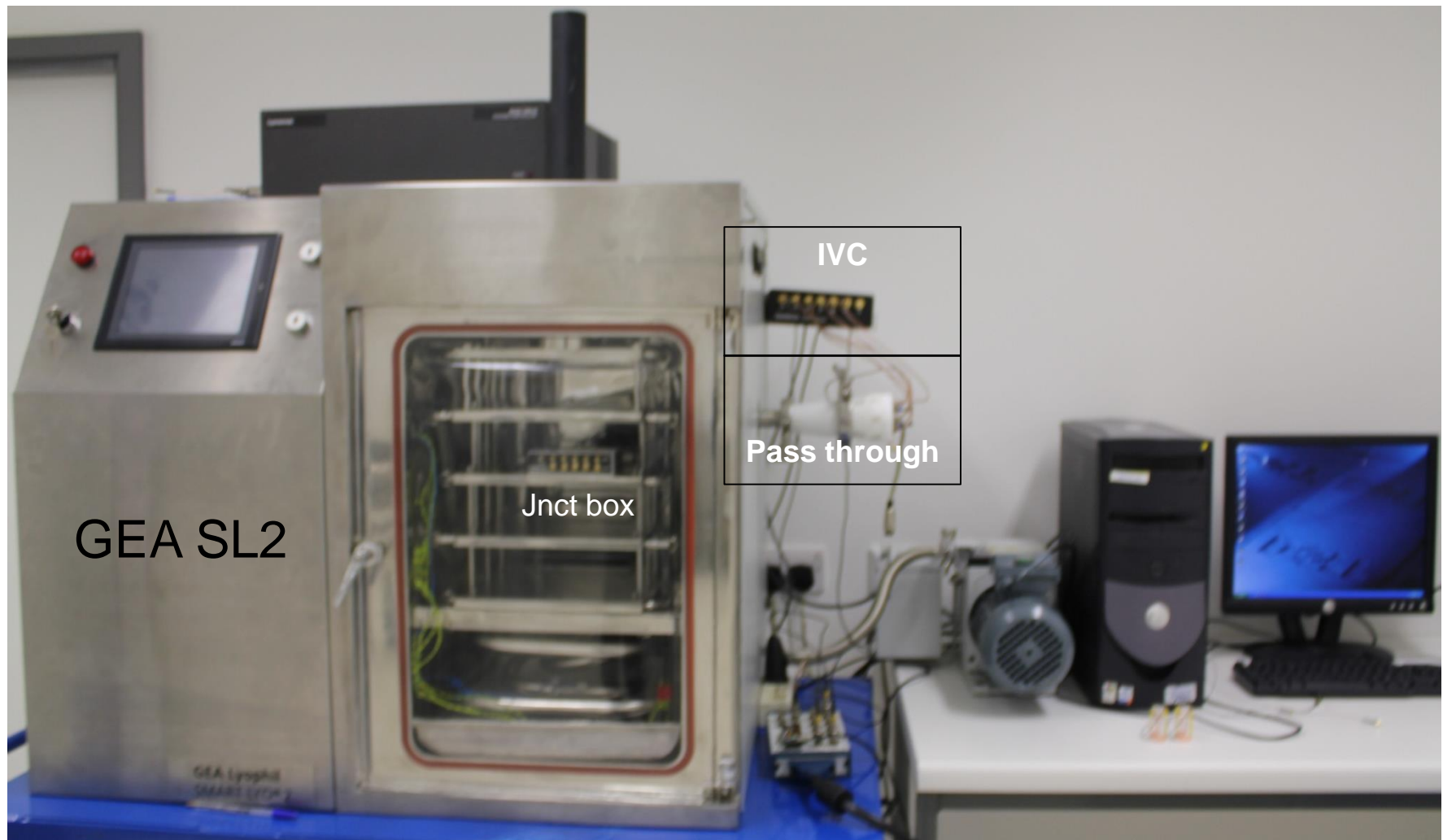
TVIS could be deployed at the scale of a vial or a population of vials

The mesoscale is accessible by assessing the temperature dependence of the impedance

The challenge is to find ways in which these two attributes may be developed so that it becomes possible to bridge the scales (molecular to macroscopic signatures)

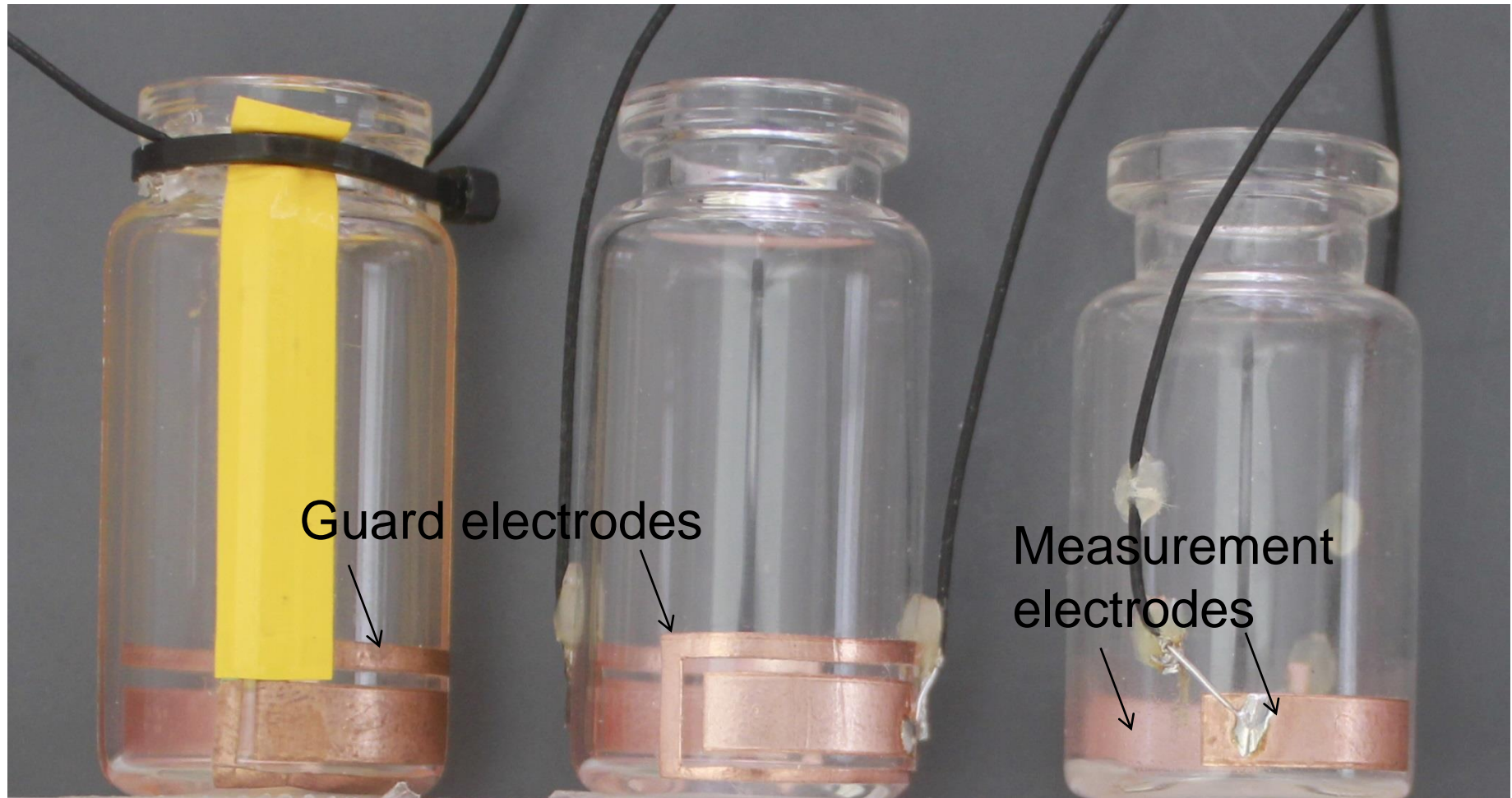


# Through Vial Impedance Spectroscopy

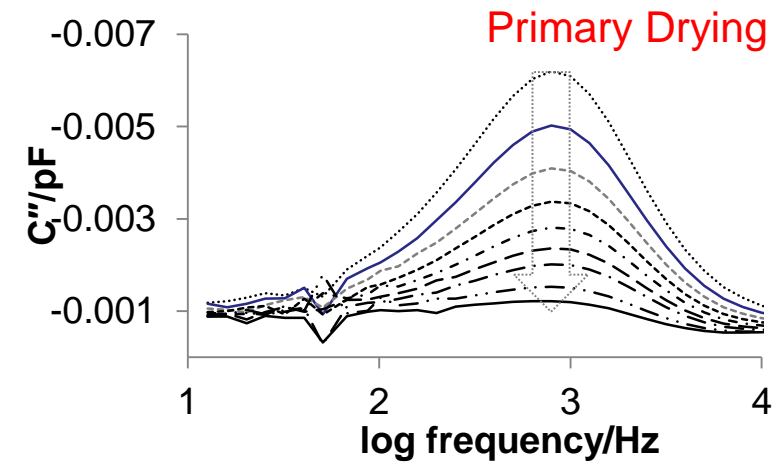
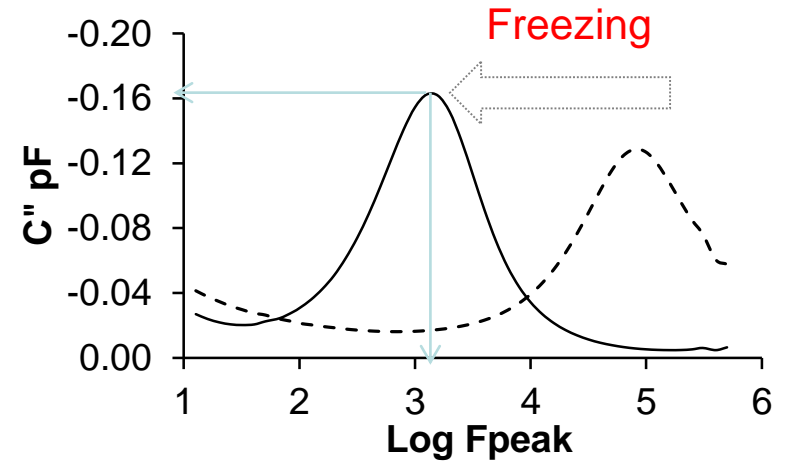
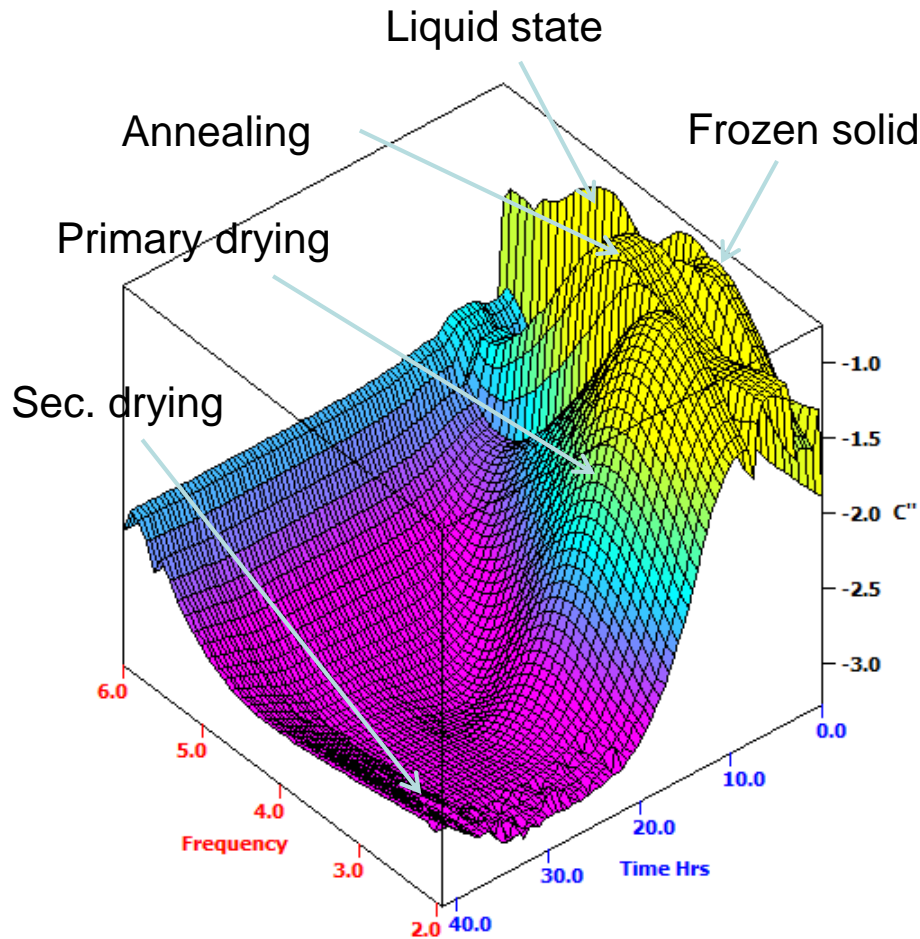




# Vial designs

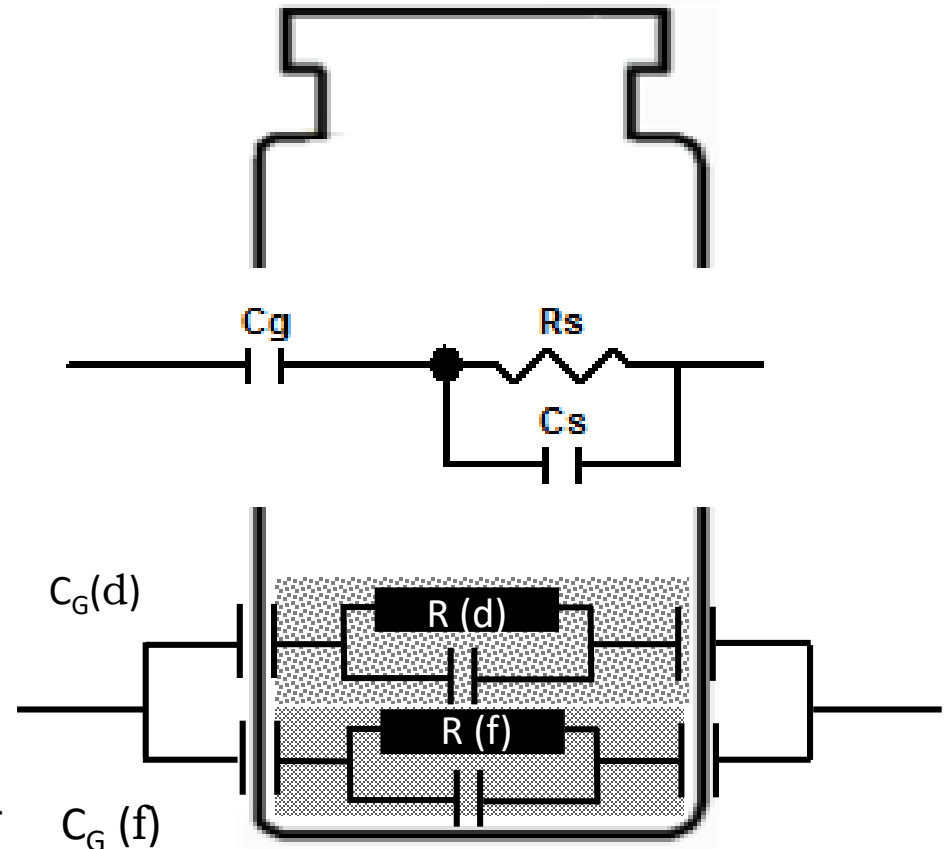


# TVIS response surface



# Through Vial Impedance Spectroscopy (TVIS)

- Electrodes attached to the external surface of a vial (either across the vial or on one side) or placed above the vial
- Composite impedance of the system depends on the size, position and orientation of the electrodes
- The sample has both resistive and capacitive properties whereas the container and any air space between the sample and the electrodes is predominantly capacitive in nature
- A typical circuit model would therefore be a capacitor modelling the glass wall (and any air space) and a parallel combination of a resistor and a capacitor modelling the electrical properties of the sample.



The impedance of the model can be calculated from the following equation

$$Z^* = \frac{1}{i\omega C^*} = \frac{1}{i\omega C_G} + \frac{1}{\frac{1}{R_S} + i\omega C_S}$$

which re-arranges to

$$Z^* = \frac{1}{i\omega C_G} + \frac{R_S}{1 + i\omega R_S C_S} = \frac{1 + i\omega R_S(C_G + C_S)}{i\omega C_G - \omega^2 R_S C_G C_S}$$

Impedance can also be expressed in terms of a complex capacitance

$$C^* = C' + C'' = \frac{1}{i\omega Z^*} = \frac{C_G + i\omega R_S C_G C_S}{1 + i\omega R_S(C_G + C_S)}$$

From the complex capacitance formula, the expressions for real and imaginary capacitance can be calculated to explain the origin of interfacial polarization peak. This achieved by multiplying the nominator and denominator by the complex conjugate of the denominator and by grouping the real ( $C'$ ) and imaginary ( $C''$ ) parts

$$C^* = \frac{1}{i\omega Z^*} = \frac{(C_G + i\omega R_S C_G C_S)(1 - i\omega R_S(C_S + C_G))}{(1 + i\omega R_S(C_S + C_G))(1 - i\omega R_S(C_S + C_G))} = \frac{C_G + \omega^2 R_S^2 C_G C_S(C_S + C_G) - i\omega R_S C_G^2}{1 + (\omega R_S(C_S + C_G))^2}$$

To obtain

$$C' = \frac{C_G + \omega^2 R_S^2 C_G C_S(C_S + C_G)}{1 + (\omega R_S(C_S + C_G))^2} \quad \text{and} \quad C'' = -\frac{\omega R_S C_G^2}{1 + (\omega R_S(C_S + C_G))^2}$$



# Real Part Capacitance

- The value of real part of capacitance at  $\omega \rightarrow 0$  is

$$C' = C_{G(fl)} = f(v_{ice})$$

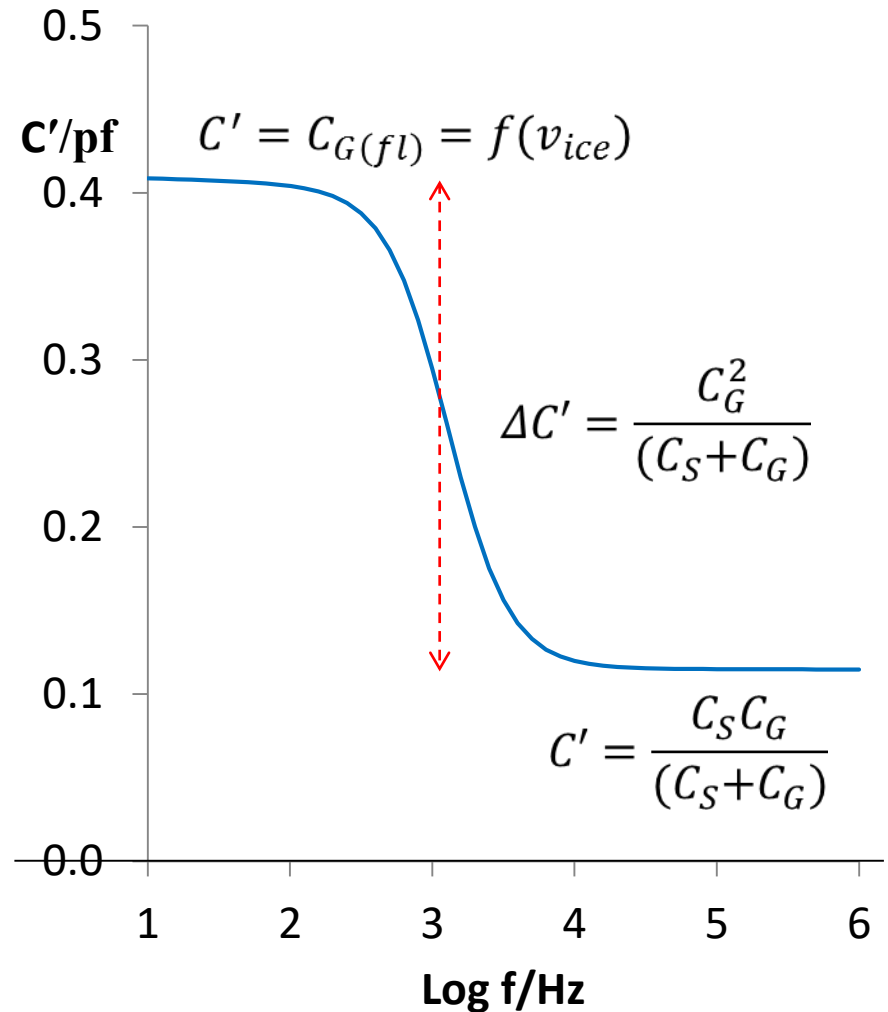
- and value at  $\omega \rightarrow \infty$

$$C' = \frac{C_S C_G}{(C_S + C_G)}$$

- It follows that the step change in capacitance is

$$\Delta C' = C_G - \frac{C_S C_G}{(C_S + C_G)}$$

$$\Delta C' = \frac{C_G^2}{(C_S + C_G)}$$



# Imaginary Part Capacitance

At  $\omega \rightarrow 0$ ,  $C'' = 0$ . As the frequency increases,  $C''$  increases to a maximum ( $C''_{max}$ ) then decreases to 0 as the frequency  $\omega \rightarrow \infty$

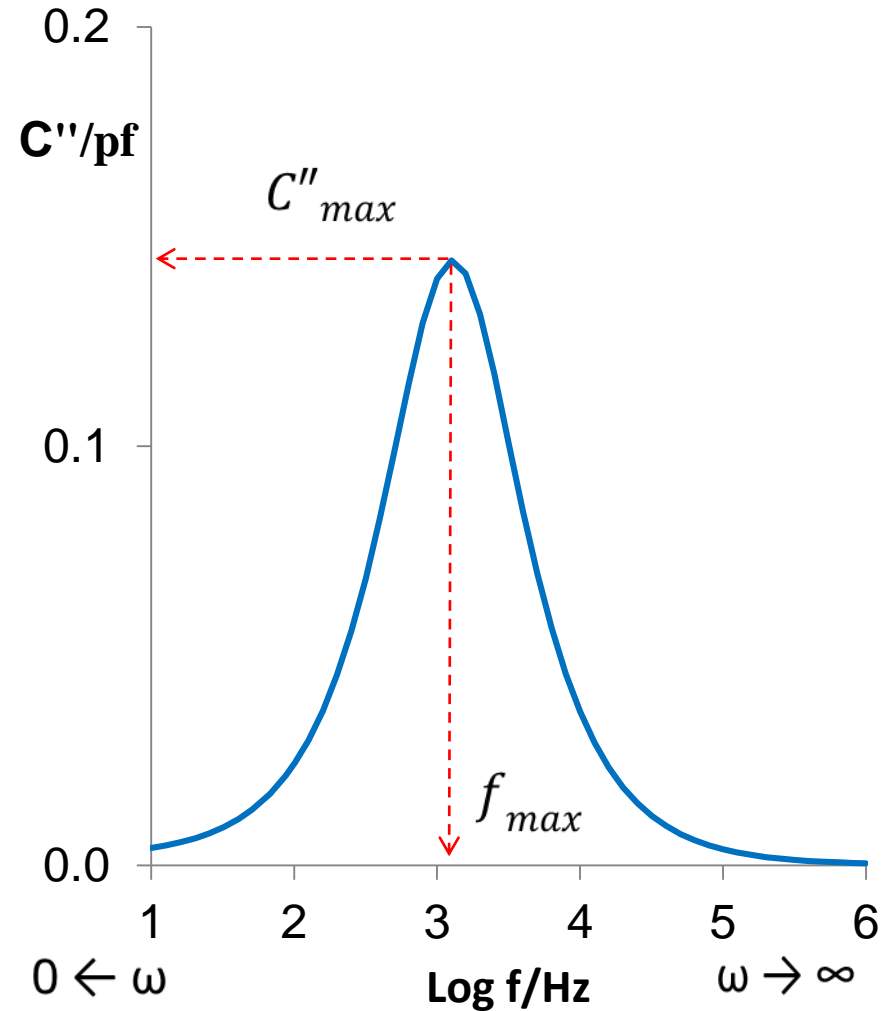
$$C''_{max} = \frac{C_G^2}{2(C_S + C_G)}$$

at a frequency of

$$\omega_{max} = \frac{1}{R(C_S + C_G)} \text{ in radians}$$

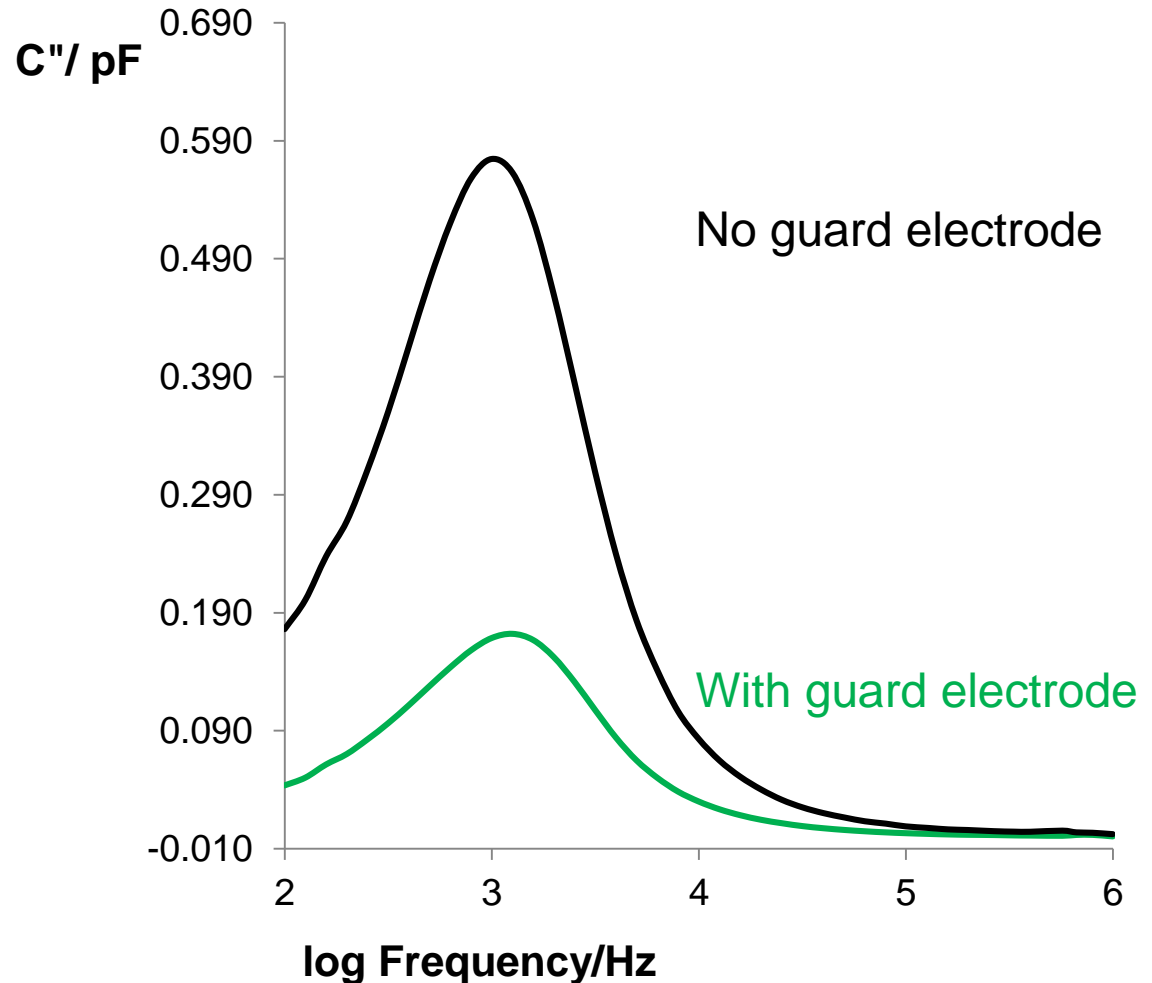
Or

$$f_{max} = \frac{1}{2\pi R(C_S + C_G)} \text{ in cycles per second}$$



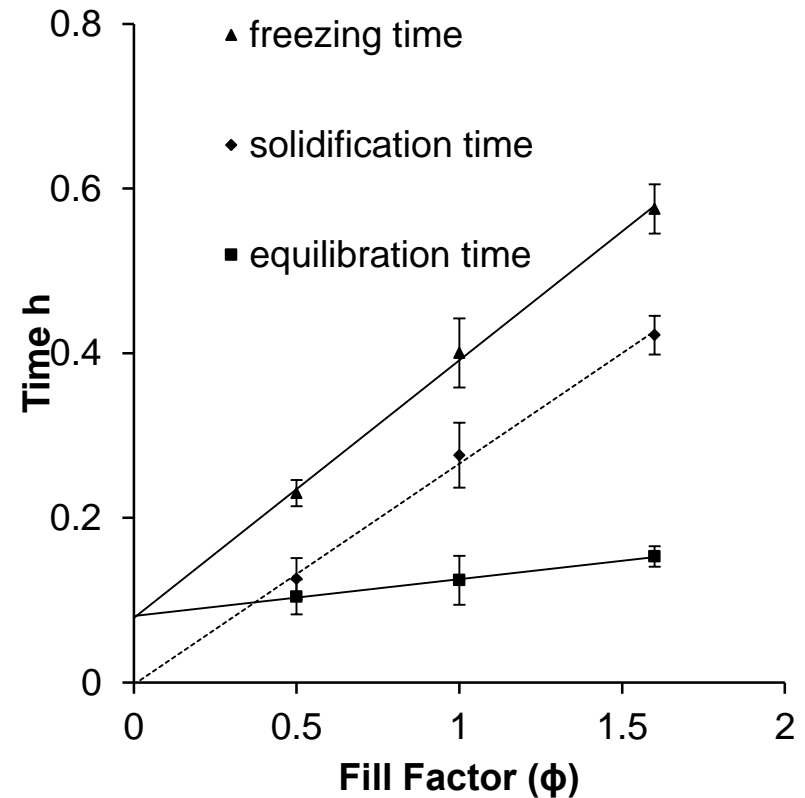
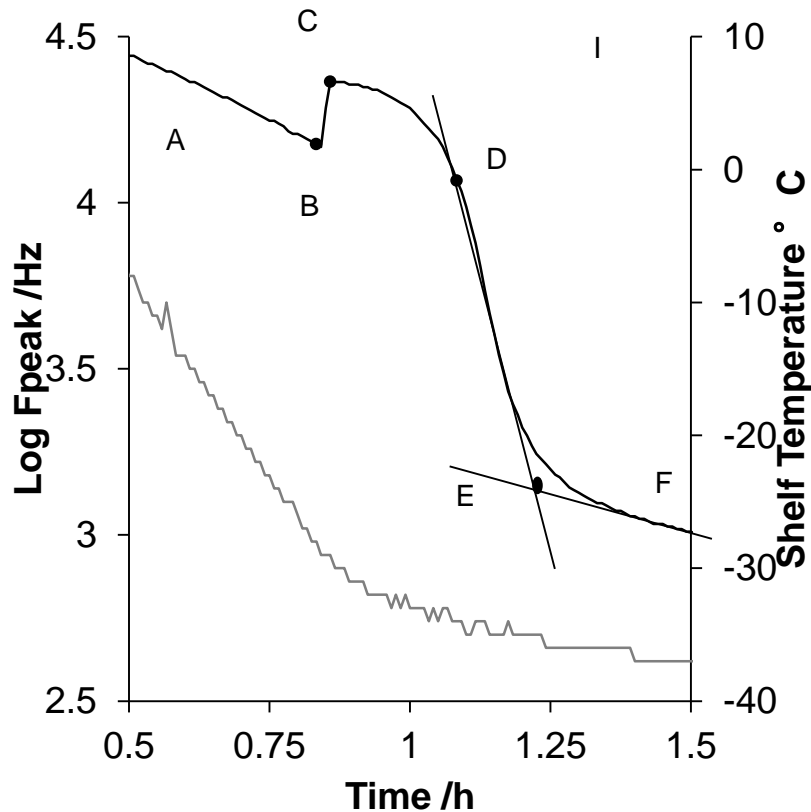
# Removal of the guard electrode

- Right shows example spectra of frozen distilled water using two different TVIS vials, one with guard electrodes and the other without
- Removal of guard electrodes has increased the amplitude of pseudo-relaxation peak almost three times with respect to corresponding peak with guard electrodes.



# Product Characterization – Ice formation

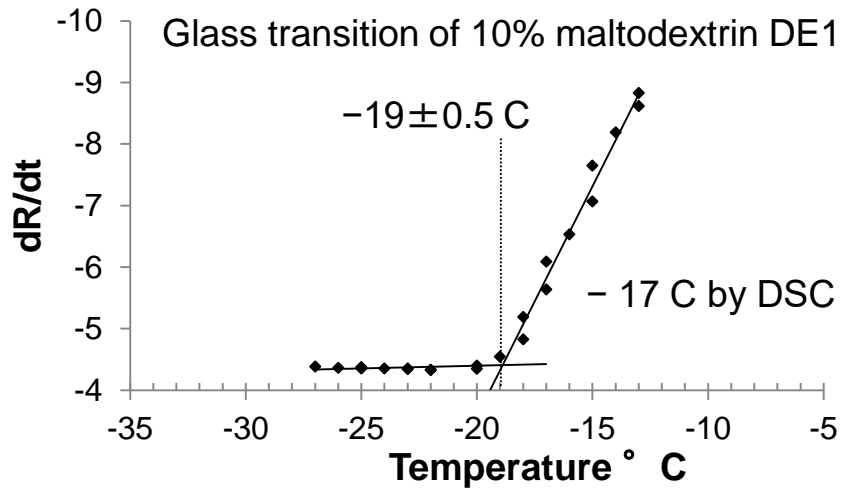
$F_{\text{peak}}$  profile records freezing step (B-E) which progress through 2 discrete stages; solidification(B-D) and equilibration(D-E). Time duration for the former increase with the fill height while the latter remain broadly unchanged as it is related to thermal coefficient of the vial base *Smith G et al (2014) AAPS PharmSciTech 15(2): 261–269*



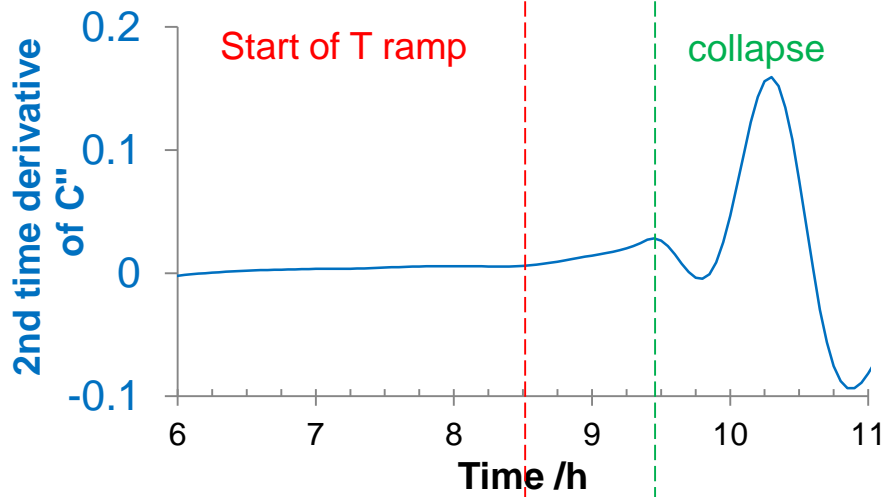
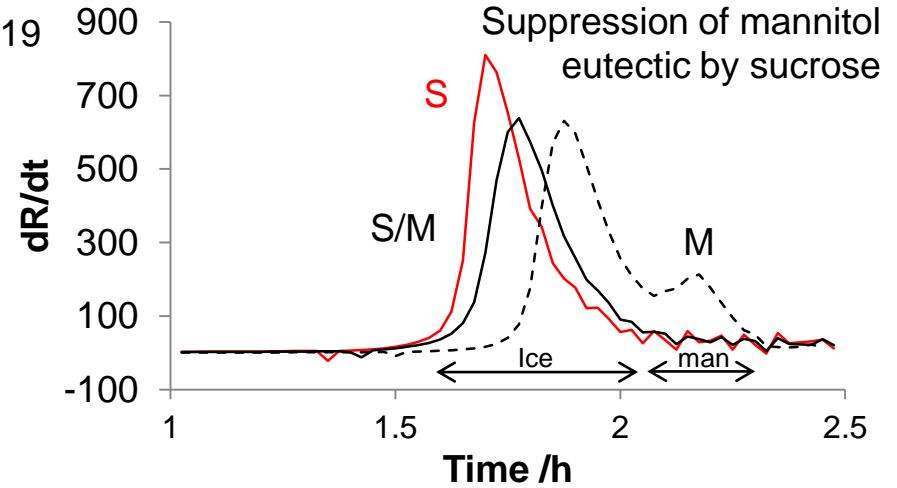


# Product Characterization : Glass transition, Eutectic Crystallization, Collapse

Smith G et al (2013) Eur J Pharm Biopharm 85 (3):1130-40



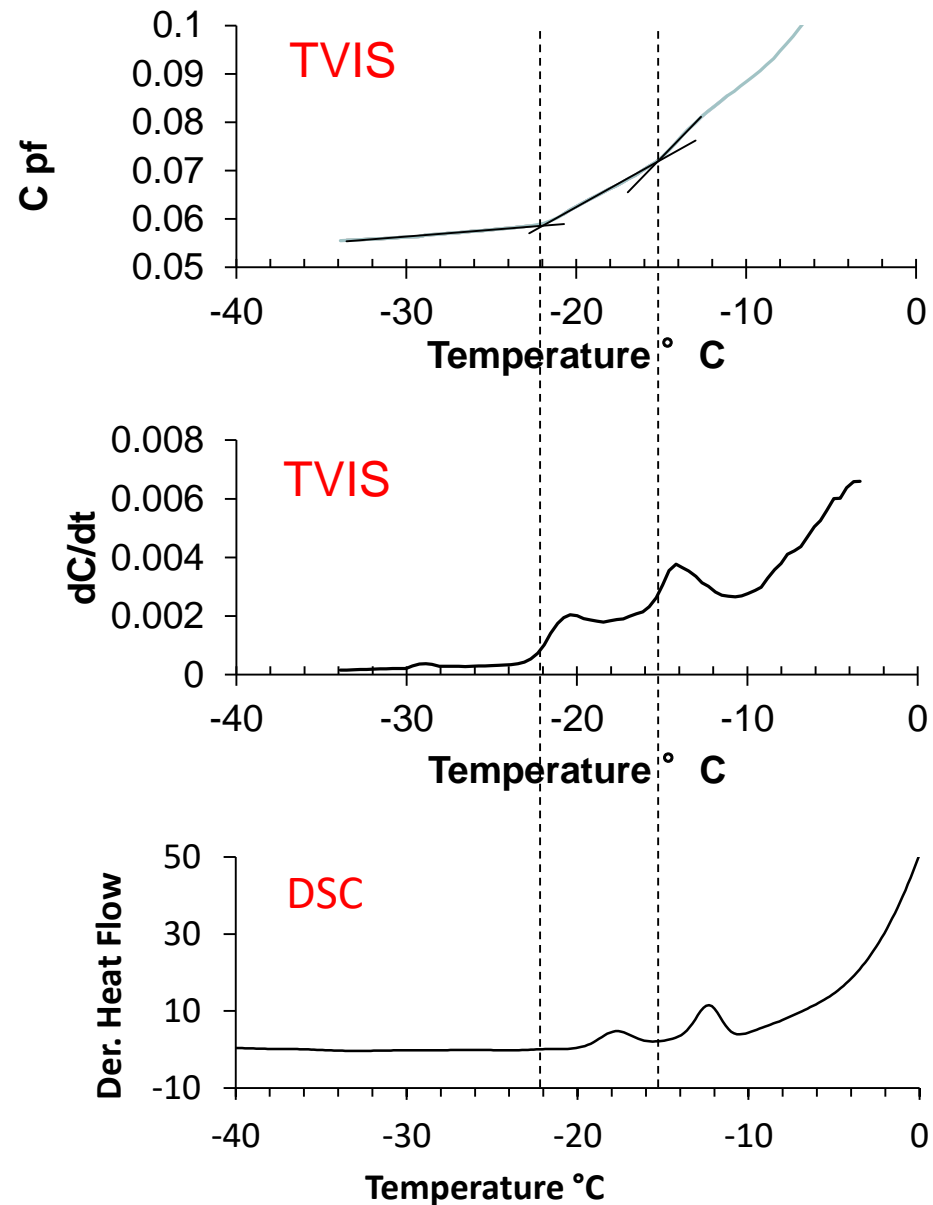
Arshad MS et al (2014) Eur J Pharm Biopharm 87(3):598-605



Smith G et al (2014) Pharmaceutical Technology 38(4)

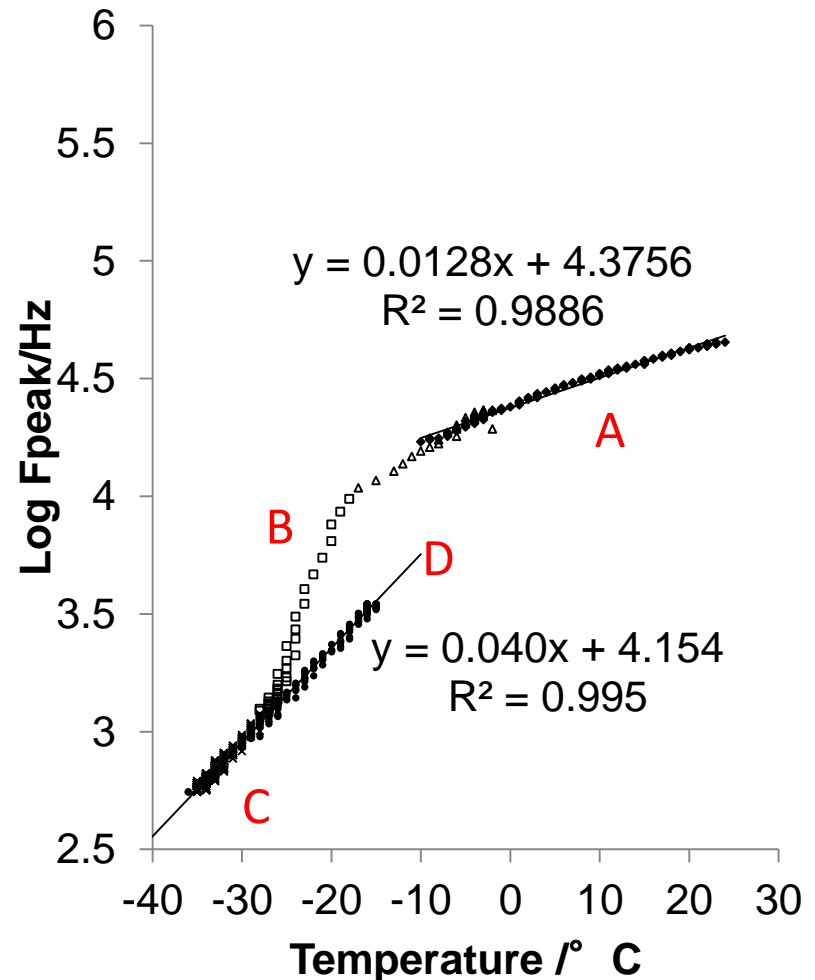
## Phase separation

- The discontinuities in the gradients of  $C$  were recorded at  $-15^{\circ}\text{C}$  and  $-22^{\circ}\text{C}$  (estimated from the inflection point) while the changes in  $R$  were less clear as the gradient changed over a longer period of time.
- The lower glass transition temperature ( $T'_G$ ) from the impedance profiles (relative to the DSC data) is a likely consequence of the slower cooling rate in the vial which might favour increased ice formation and a more concentrated unfrozen fraction.



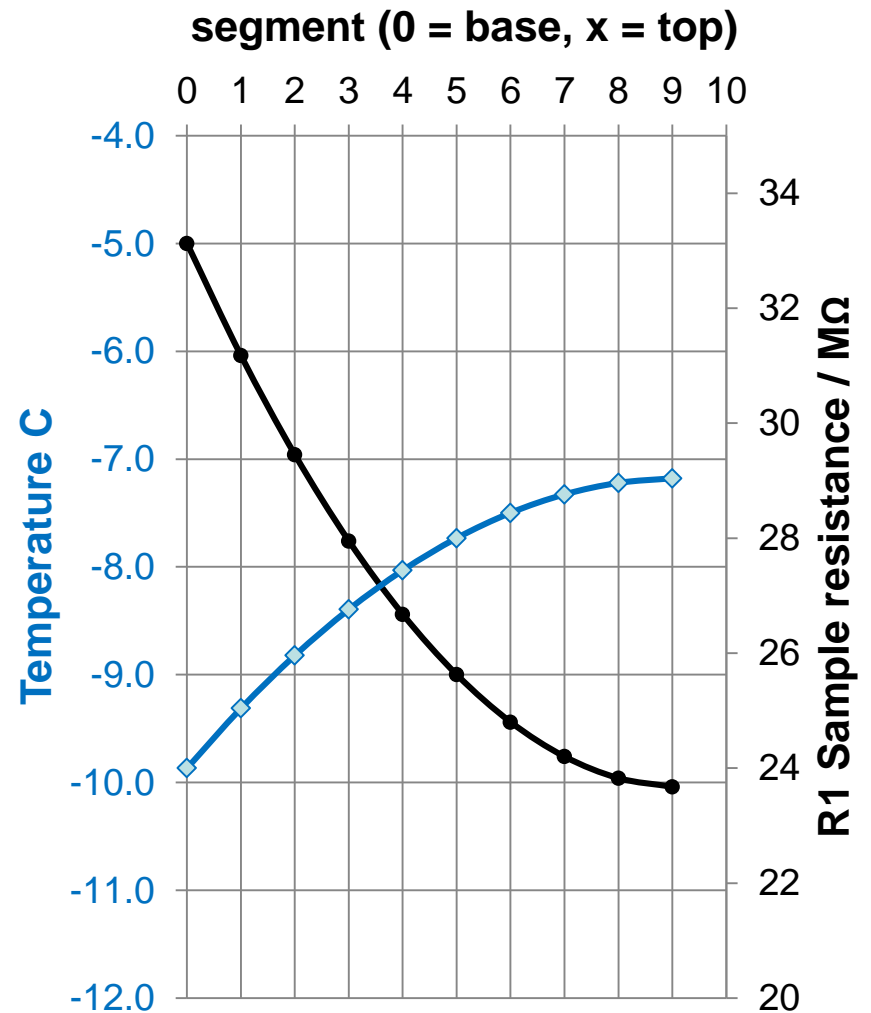
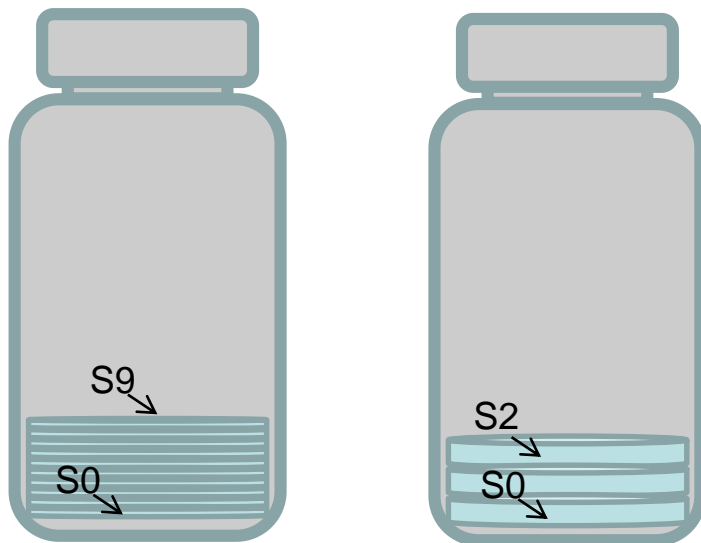
# Product Characterization : Temperature

- The  $f_{\text{peak}}$  showed a good correlation with the product temperature during product cooling (A), freezing (B) and annealing (C)
- Provided there is no change in phase, then a linear correlation exists between Log F and temperature (A, C-D)
- Temperature coefficient for log  $F_{\text{peak}}$  in the frozen state (C-D) is  $\sim 0.04$  which is approx. x3 of the temperature coefficient in the solution state



# Model of temperature profile within vial

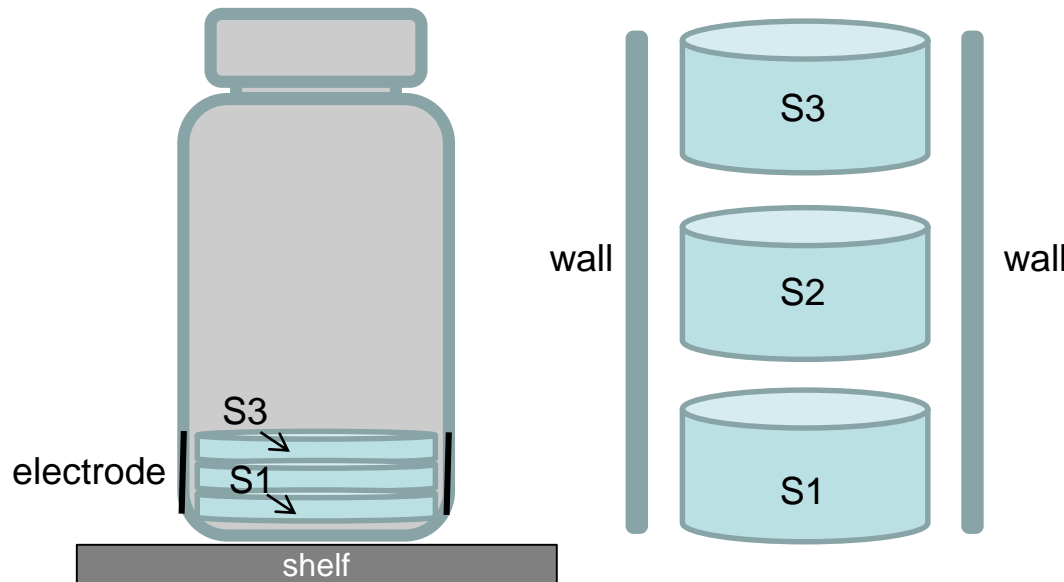
- Divide mass of frozen solid into segments (0 to 2, or 0 to 9). Each segment is modelled by the following circuit



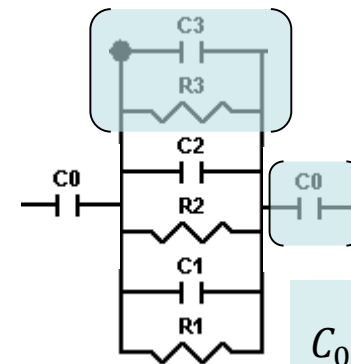


# Contact electrode : Parallel elements

- Positioning the contact electrode on the walls surrounding the sample means that the sample segments ( $n = S1-3$ ) are presented in parallel with one another, but in series with the wall impedance



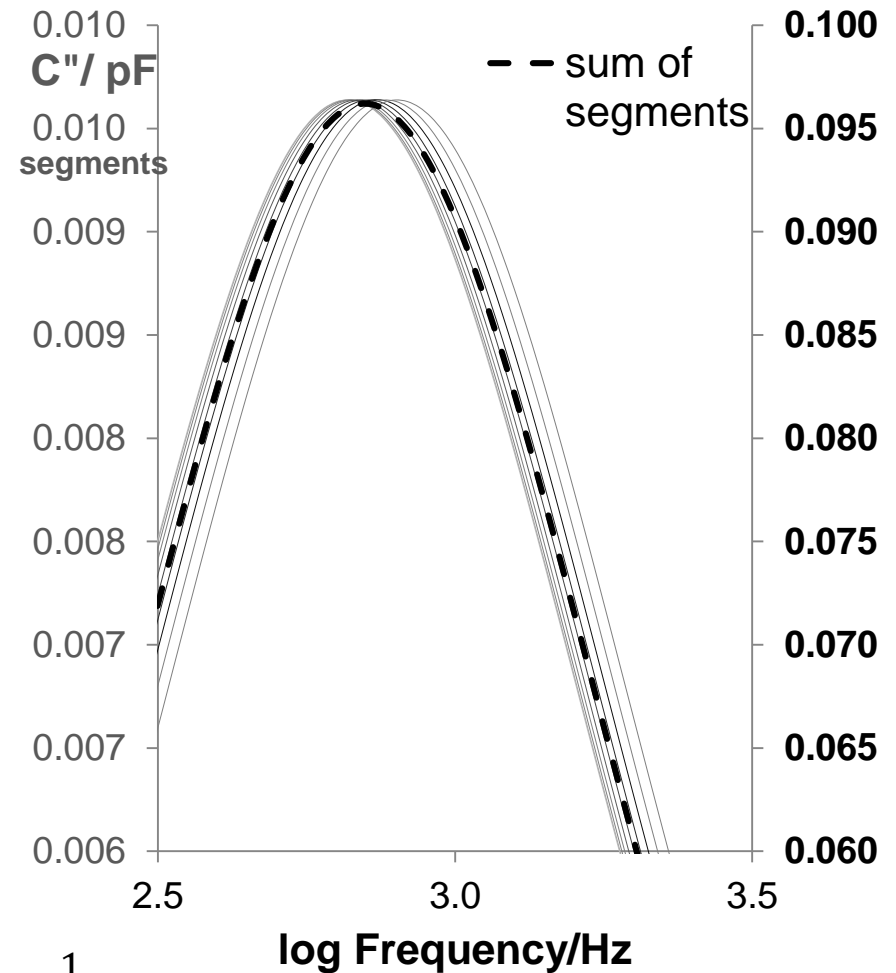
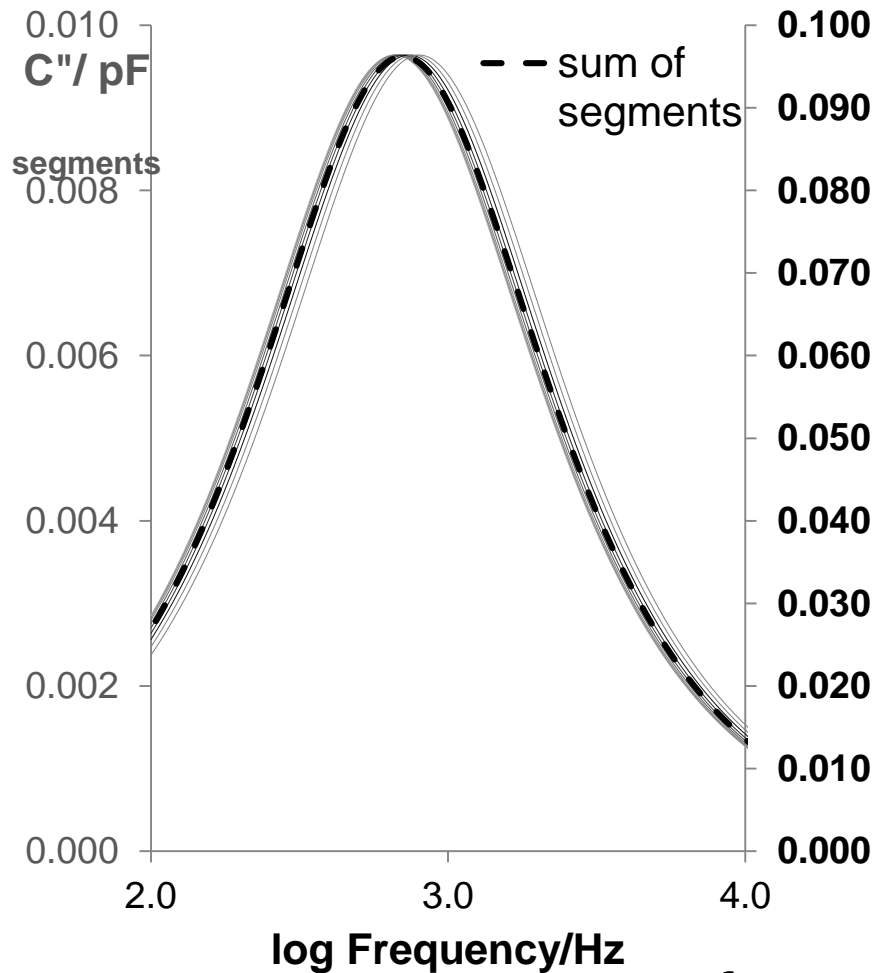
$$C_n^* (i\omega) = \frac{1}{R_n} + i\omega C_n \quad (n = 1 \text{ to } 3)$$



$$C_0^* (i\omega) = \frac{1}{i\omega C_0}$$

$$C_s^* (i\omega) = C_1^* (i\omega) + C_2^* (i\omega) + C_3^* (i\omega)$$

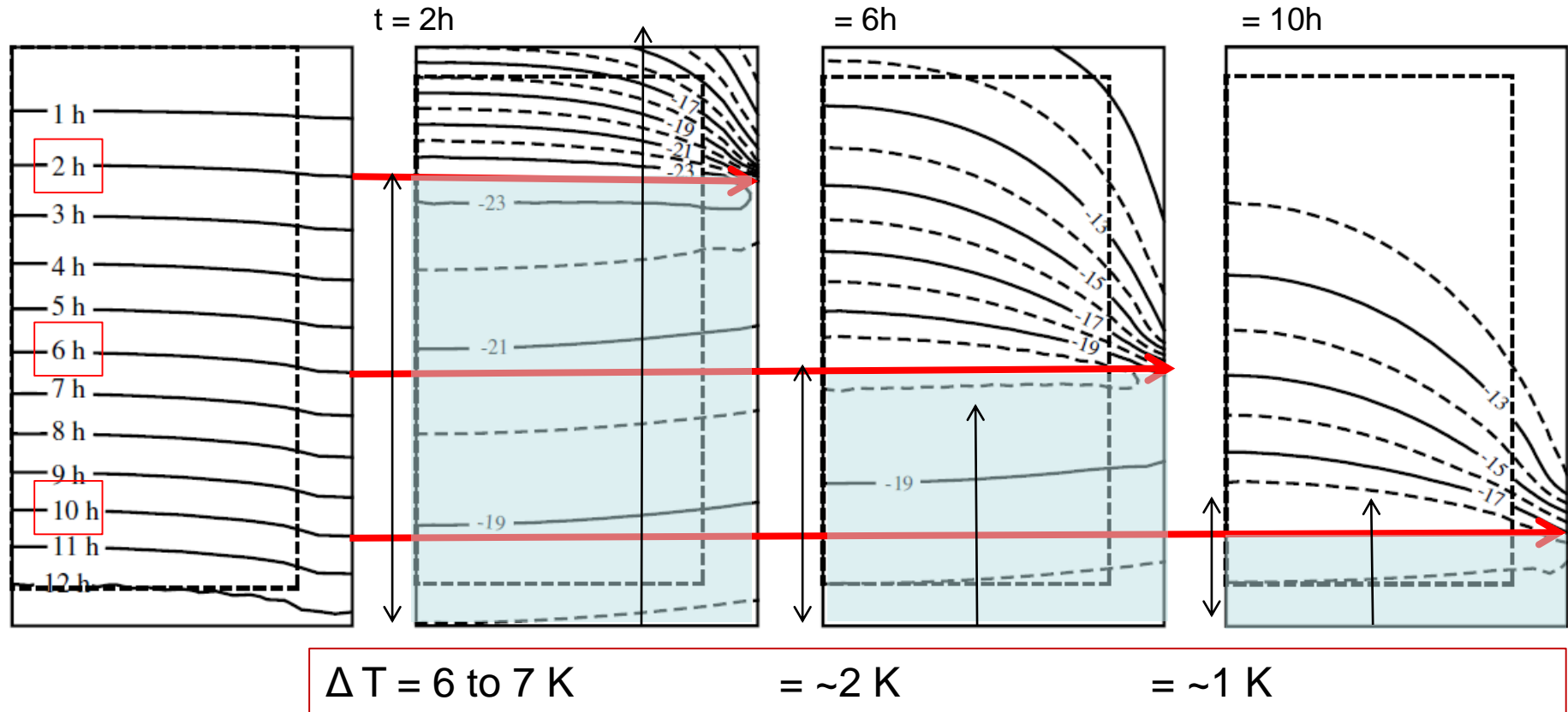
# Side electrodes



$$f_{max} = \frac{1}{2\pi R(C_S + C_G)}$$

# Macroscale: single vial

Temperature distribution in a vial during freeze-drying of skimmed milk  
Sung Song, C. et al

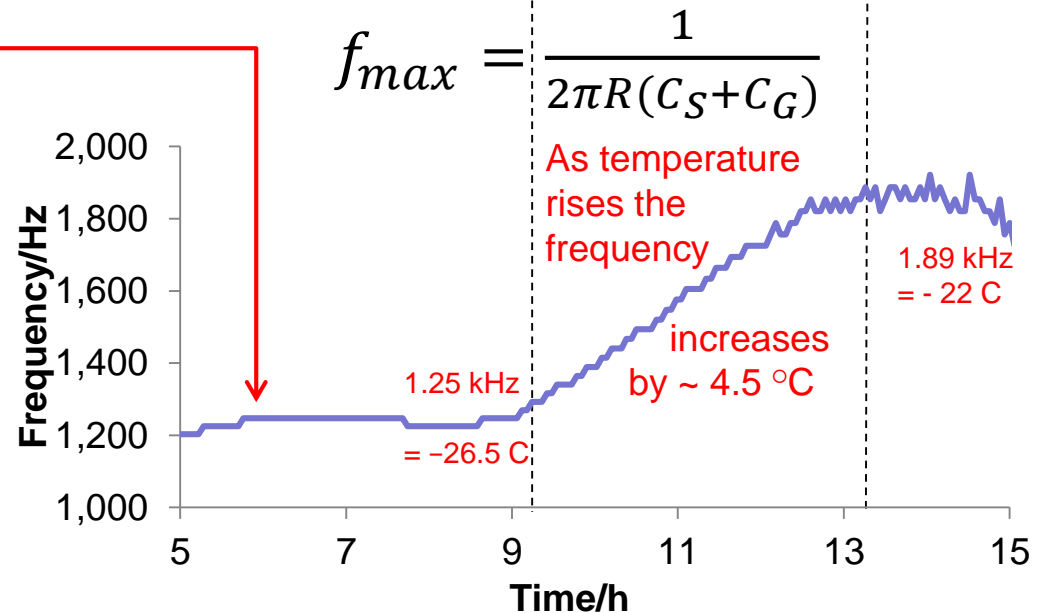
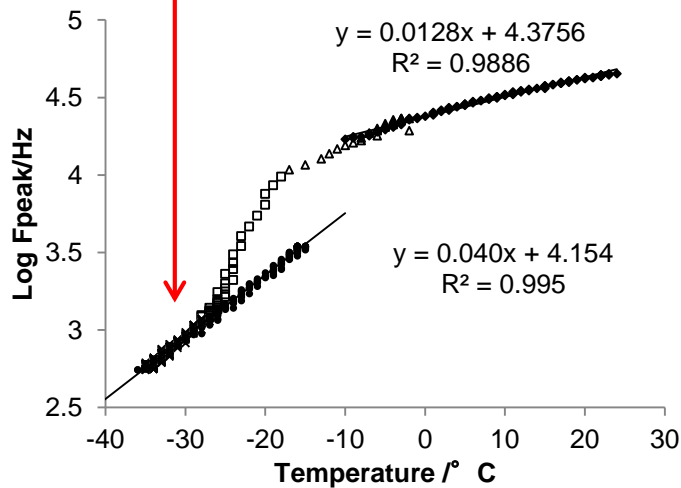
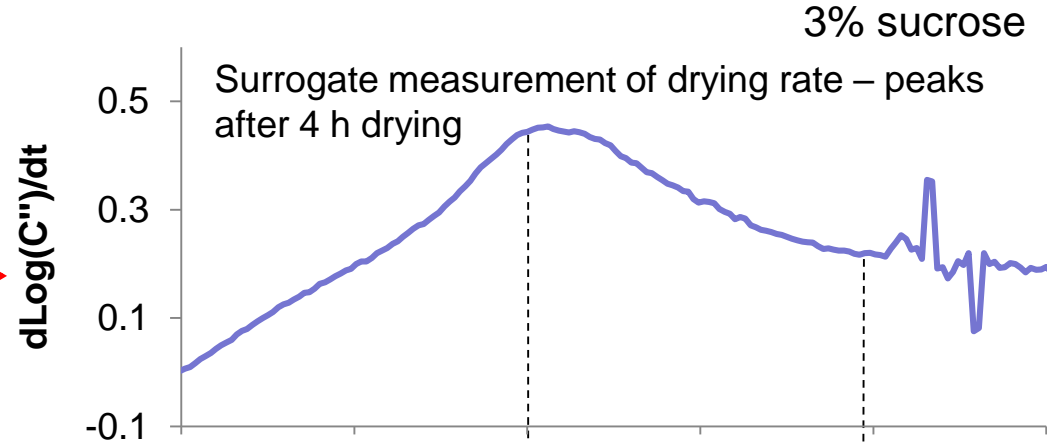


Calculated **position**  
of **sublimation**  
**interface**

Calculated **temperature profile** at time 2 h, 6 h and 10 h  
Temperature gradient in frozen layer is one dimensional – but  
in the dry layer its curved owing to the impact of wall heating

# Temperature variation in primary drying

- Temperature calibration in the frozen state
- Derivative of peak height is an indicator of drying rate
- When the drying rate peaks the temperature increases



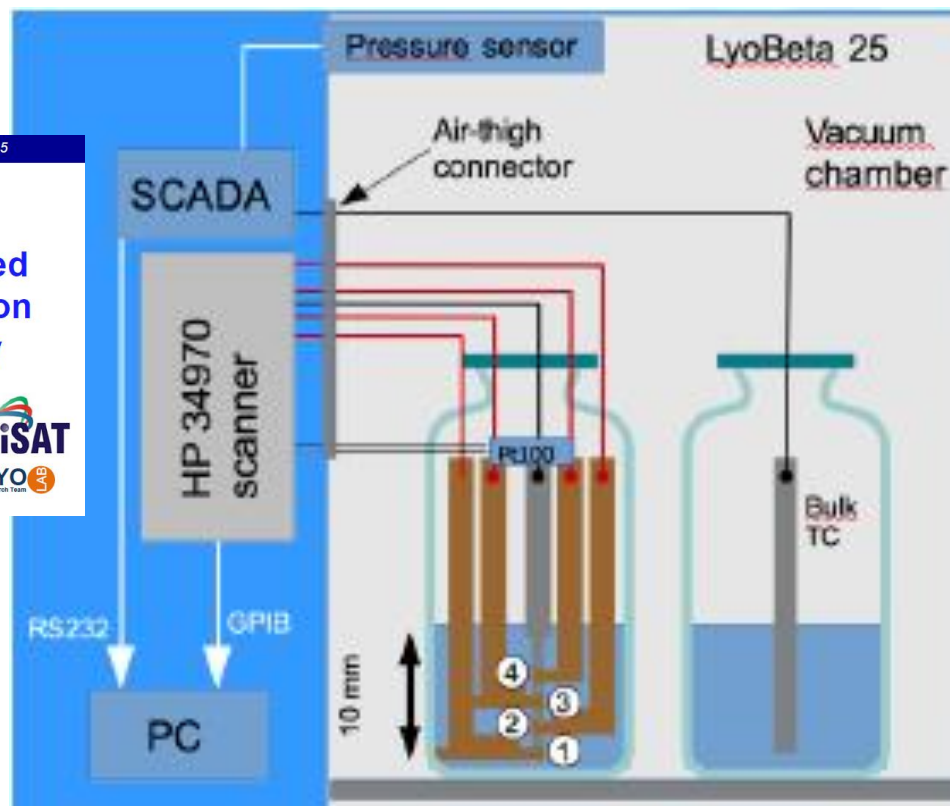


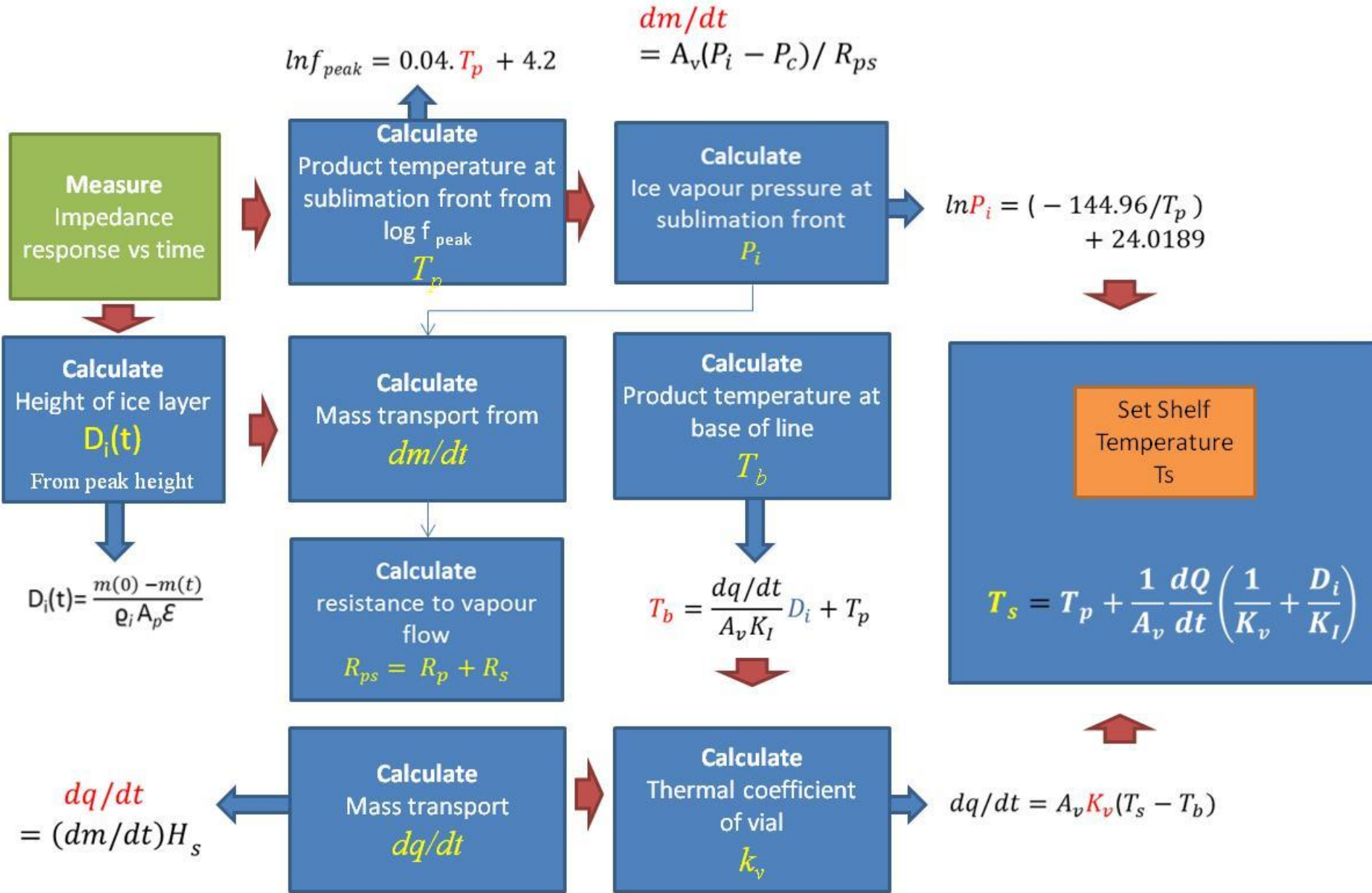
ISL-FD conference and seminar, Barcelona, Spain, 06-10 July 2015

## Effect of the Vacuum Induced Nucleation on process and on final product homogeneity



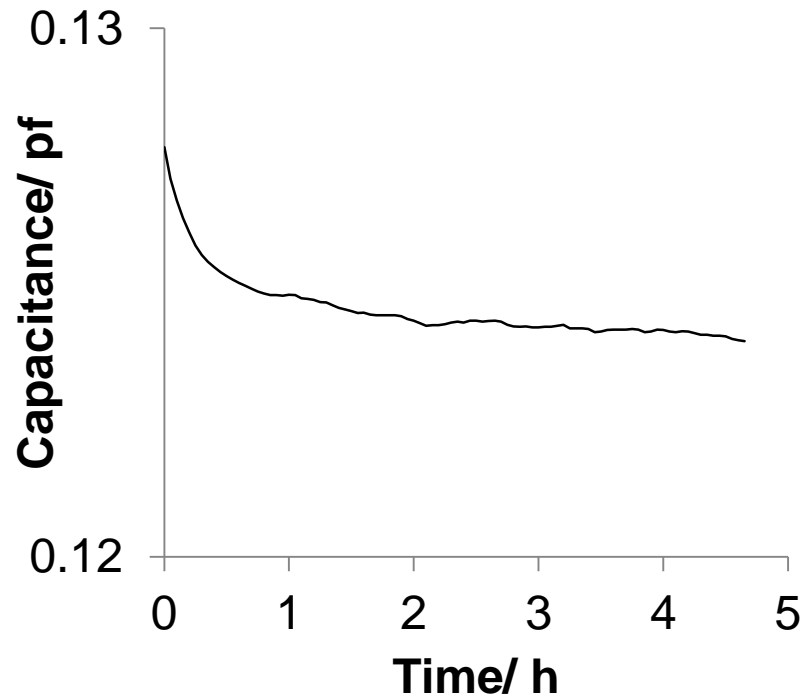
Irene Oddone  
Department of Applied Science and Technology  
Institute of Chemical Engineering  
Politecnico di Torino



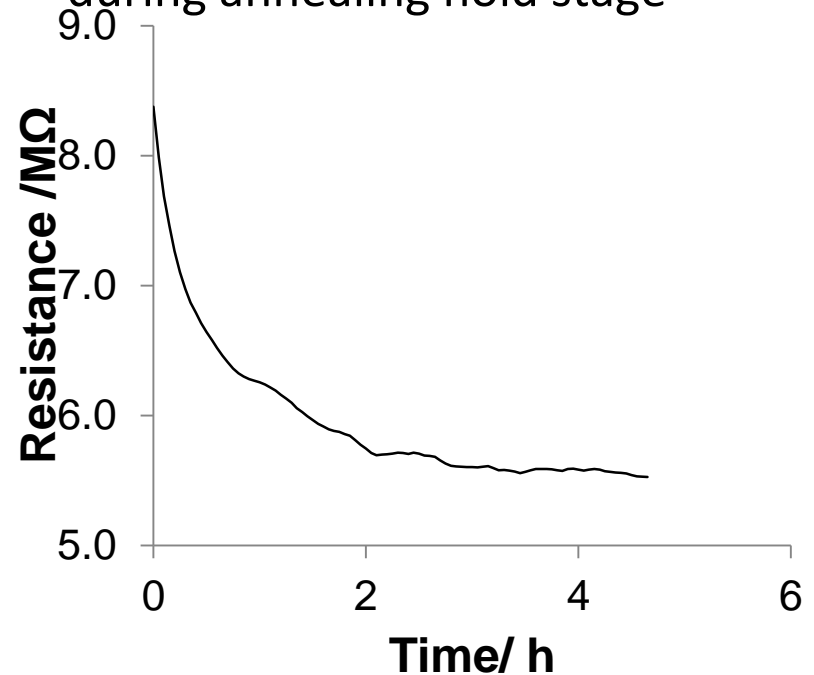


# Maltodextrin DE19 10% w/v Annealing

- Capacitance decrease only 3%



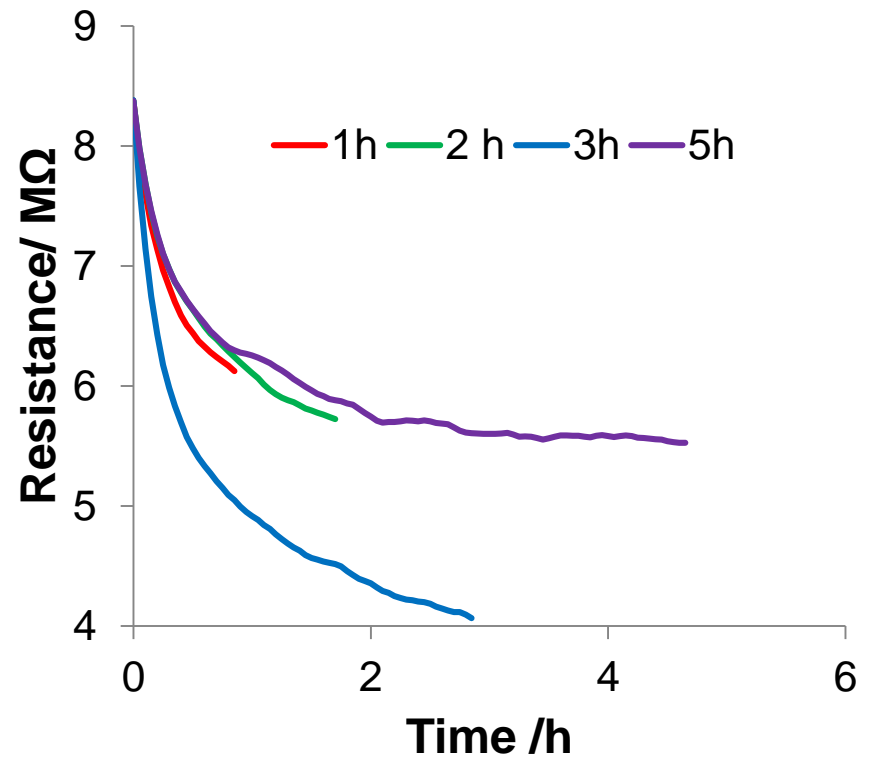
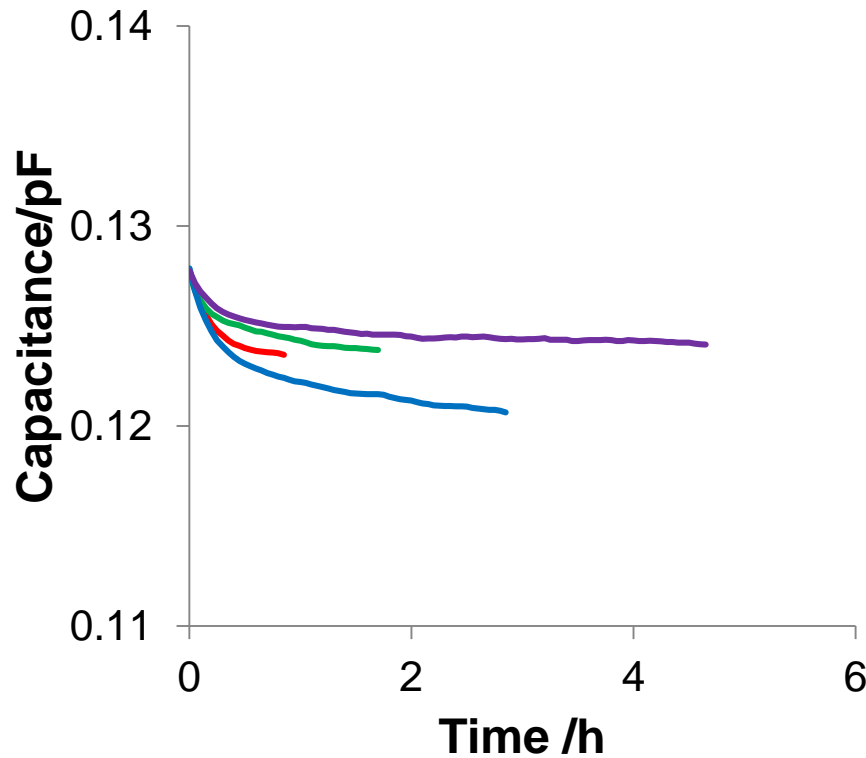
- Resistance decreases by approx. 30% during annealing hold stage



Simplification of the unfrozen mass by recrystallization effectively lowers the electrical resistance

Smith, G. et al (2014) J Pharm Sci 103 (6) 1799–1810

# Completion of Annealing (Maltodextrin 10% w/v)



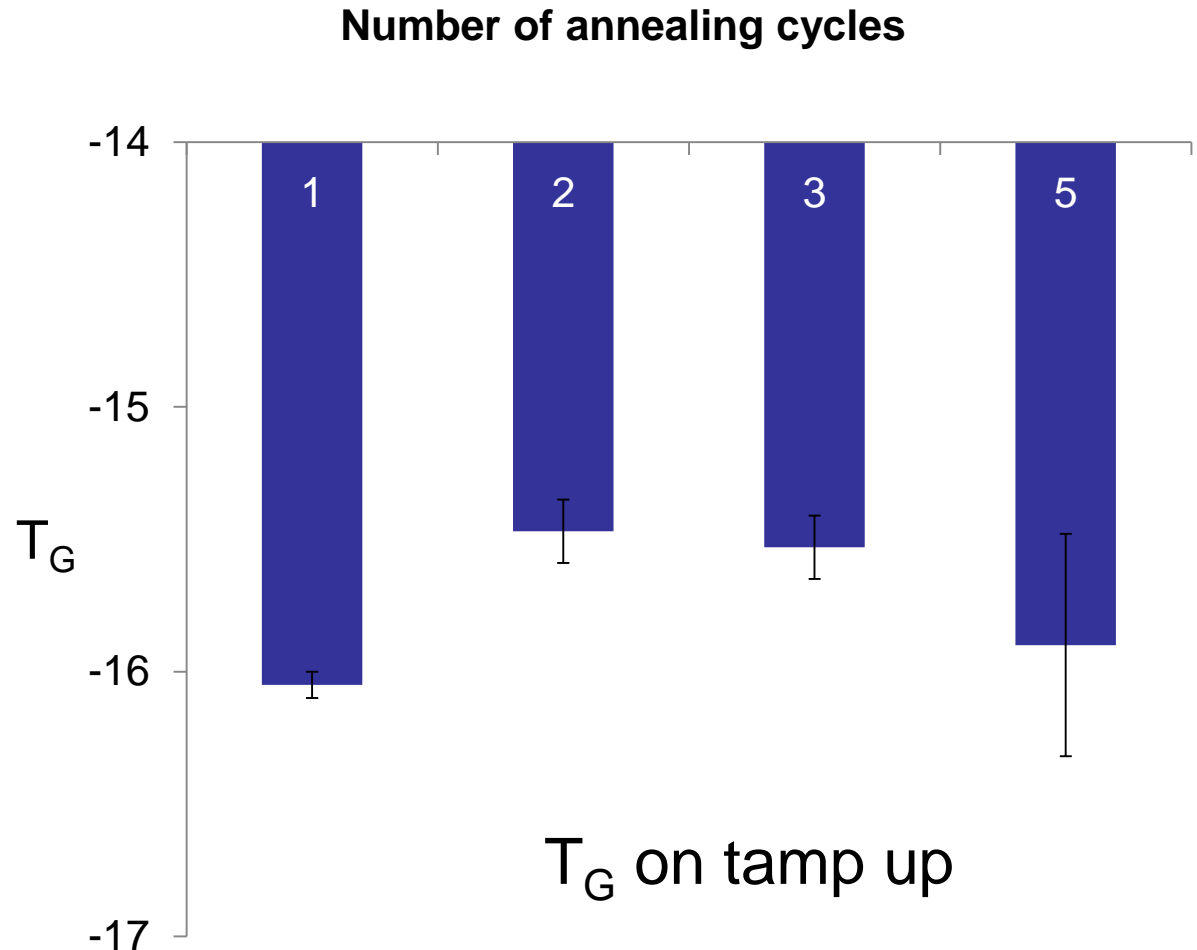
The capacitance of the formulation changes minimally while the resistance changes significantly and plateaus at 3-4 h

Simplification of the unfrozen mass by recrystallization effectively lowers the electrical resistance (i.e. recrystallization)

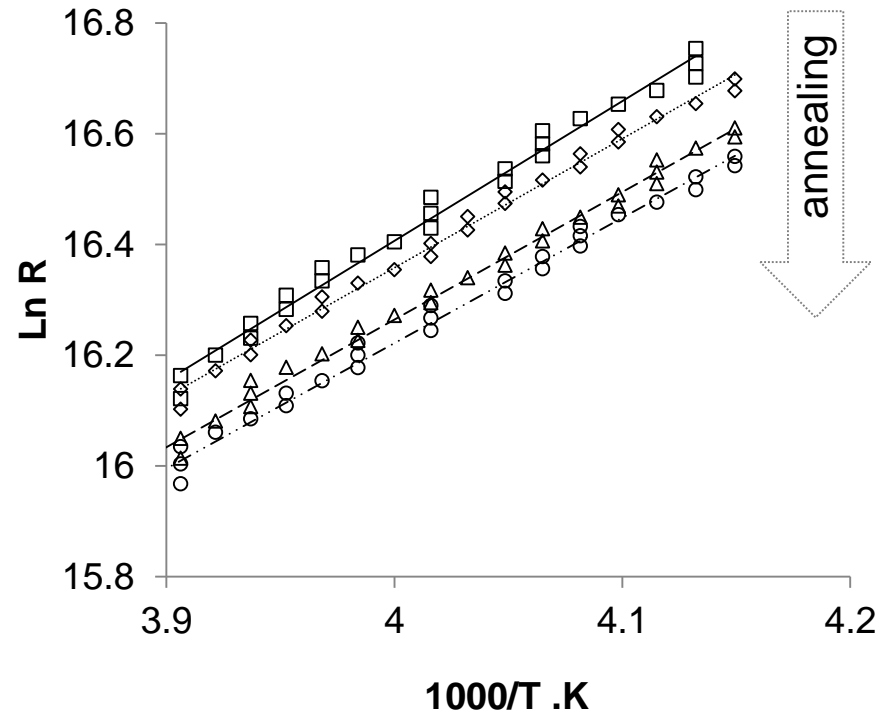
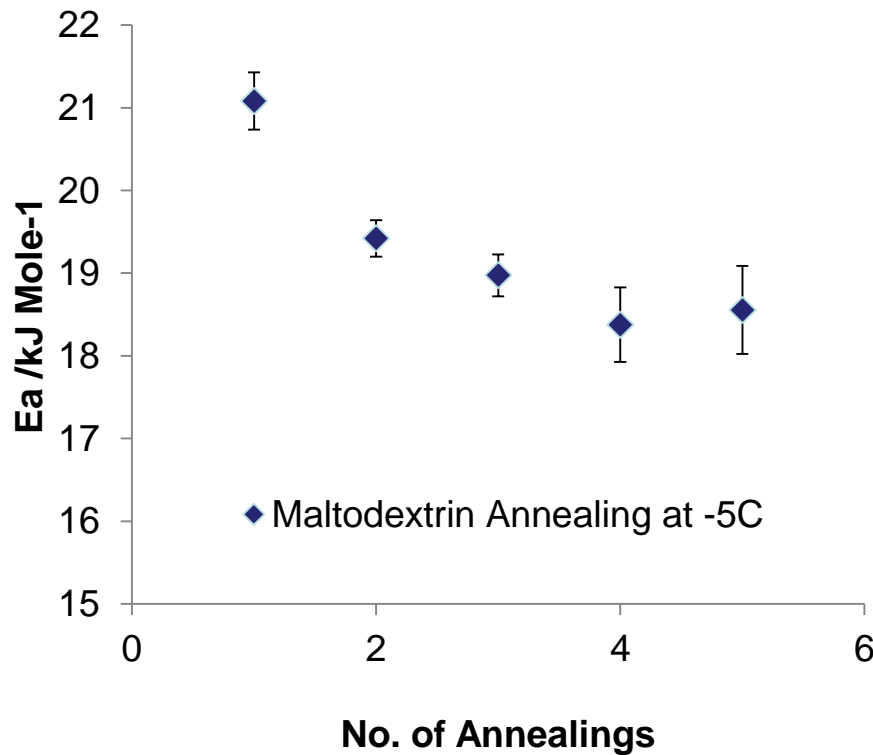


# Glass transition on annealing

- There are no appreciable differences in  $T_G$  on both ramp up and ramp down suggesting that the concentration of the unfrozen fraction does not change with annealing

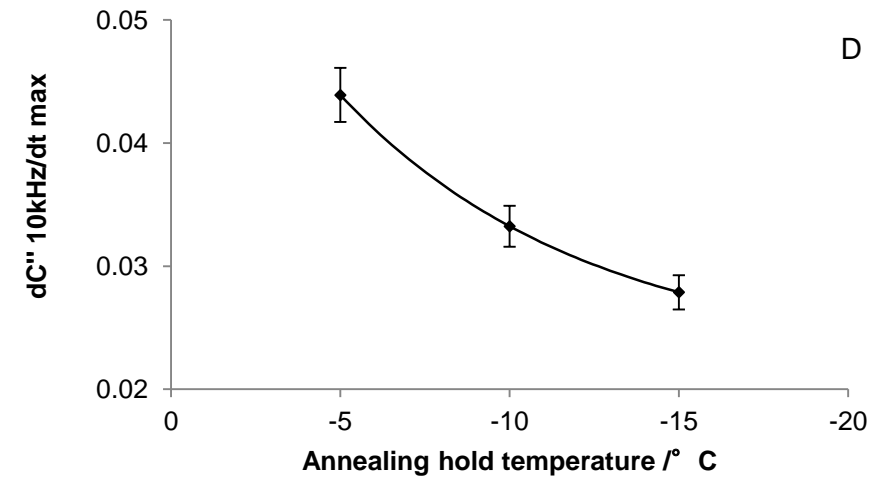
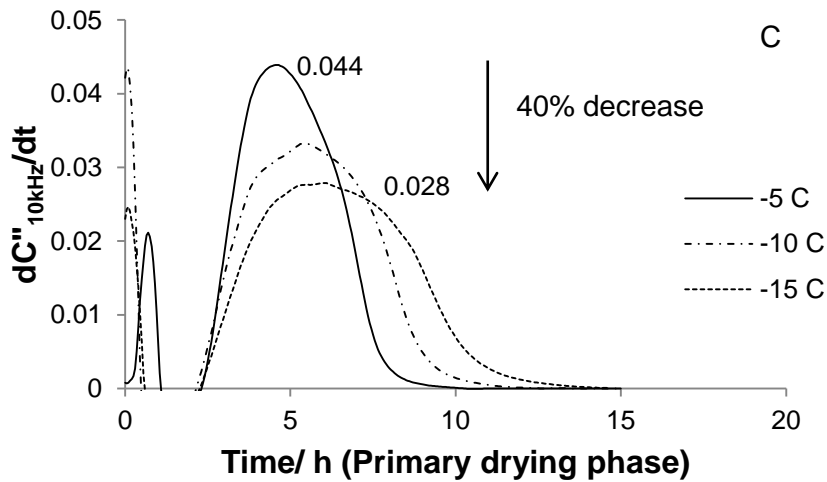
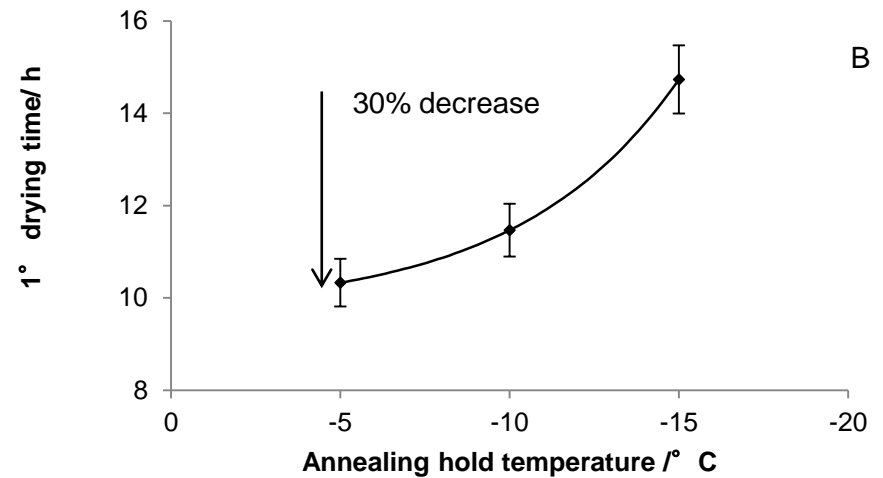
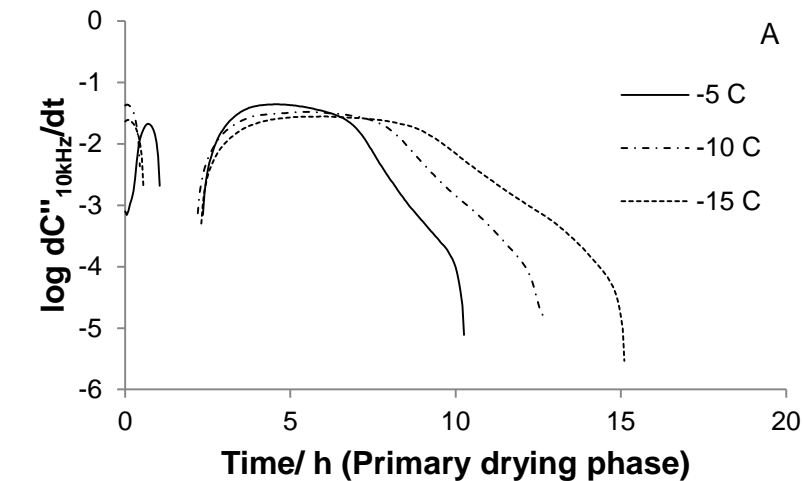


## Arrhenius Fit to describe the below Tg' resistance



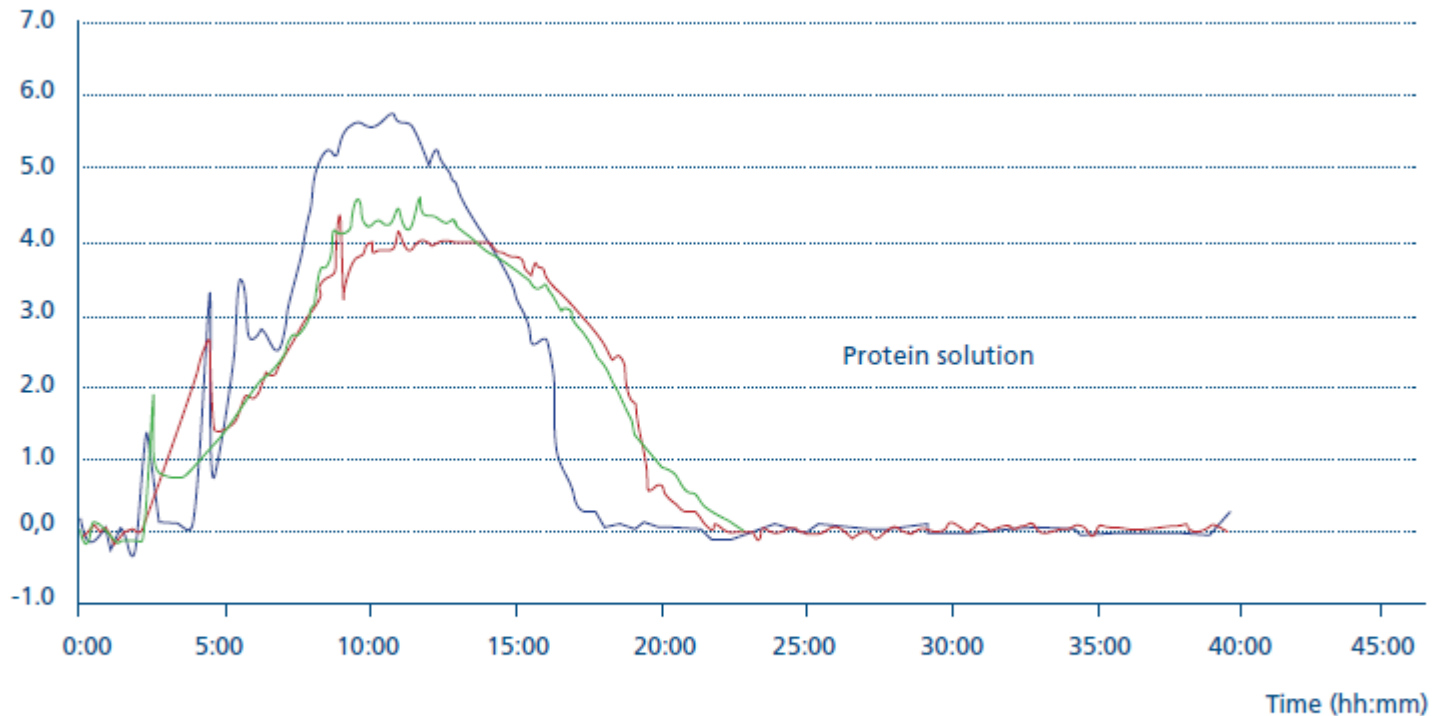
The product resistance and the activation energy for charge transport ( $E_a$ ) in the sub-Tg' temperature region decreases following annealing. The explanation is that the unfrozen fraction has a super high viscosity and that the ice structure now dominates the resistance. Reduction in  $E_a$  is again consistent with a simplification in ice structure

# Impact of annealing temperature



# Christ MICROBALANCE

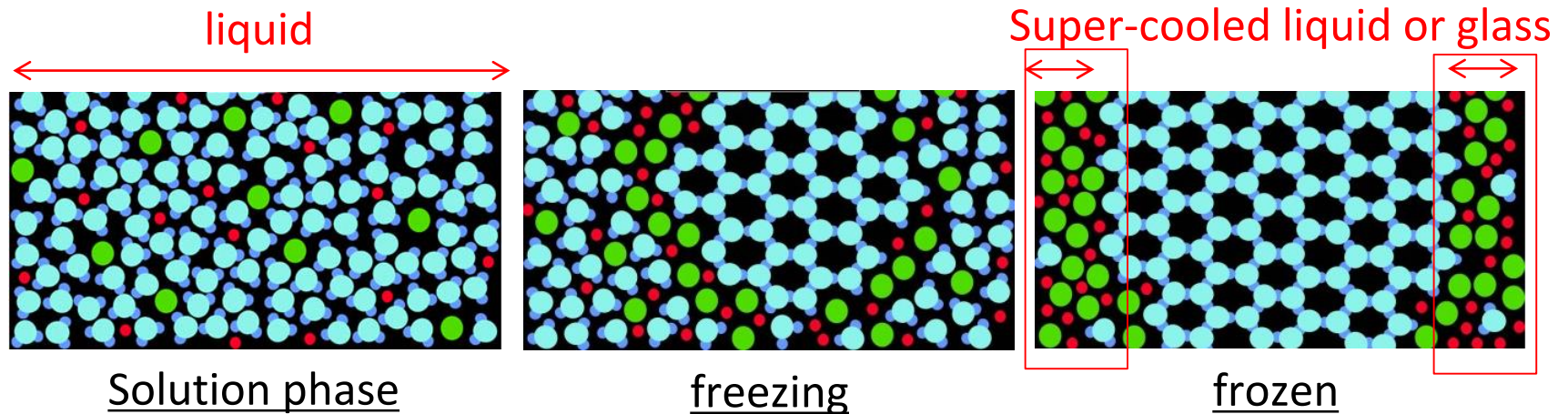
Rate of sublimation [mg/min]



- Rate of sublimation with shelf temperature -10°C and 0.1 mbar
- Rate of sublimation with shelf temperature 0°C and 0.1 mbar
- Rate of sublimation with shelf temperature 0°C and 0.05 mbar

# Meso-scale in liquids and glasses

- Liquids and glasses are known as structurally disordered materials which are often described in terms of molecular dynamics and co-operativity.

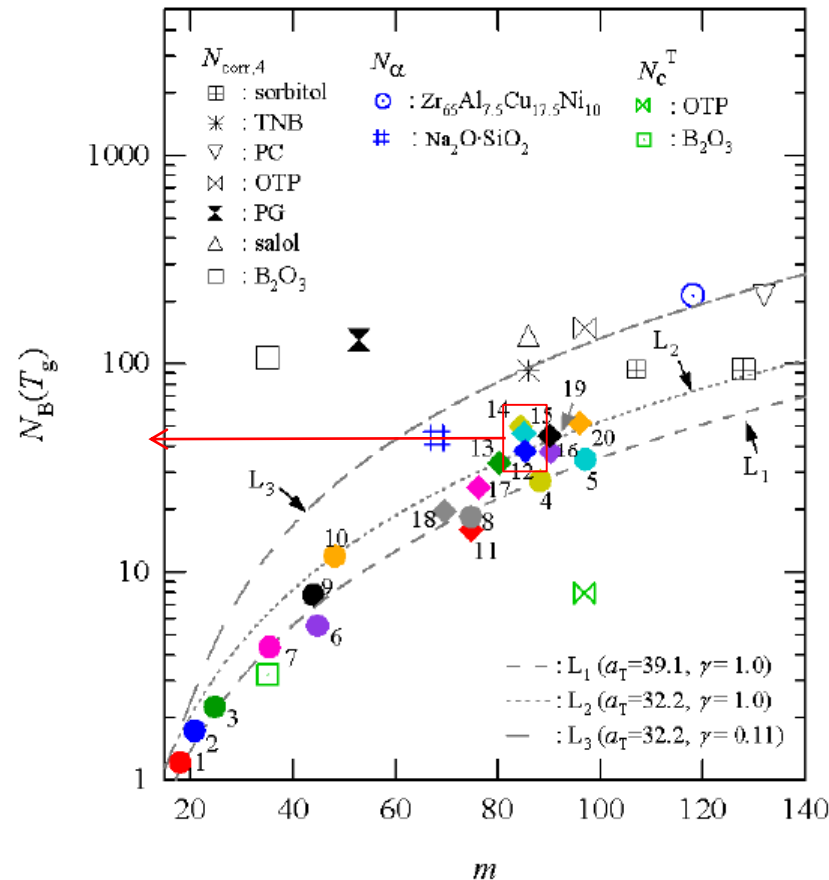


- The solid state (glass) is achieved when the temperature is reduced sufficiently to increase the viscosity to  $10^{13}$  poise
- Scale length and shape of the cooperative unit (CRR) depends on temperature. CRR can be  $\sim$  nm close to  $T_g$  and the shape compact; whereas  $>T_g$  the CRR becomes longer and more string like (Nature Physics 2, 268 - 274 (2006))
- The unfrozen fraction will inevitably contain some residual water (which in turn impacts the glass transition temperature)



# Cooperativity ( $N_B$ ) and fragility ( $m$ )

- $N_B$  is the number of molecules involved in viscous flow (i.e. the structural relaxation) at the glass transition,  $T_g$
- The fragility index is determined from the temperature dependence of the viscosity (deviation from Arrhenius)
- As the fragility index increases so does the scale length of the cooperative unit
- The model predicts that the scale length ( $\xi$ ) for the cooperative unit in a typical fragile system is in the region of 1-3 nm.

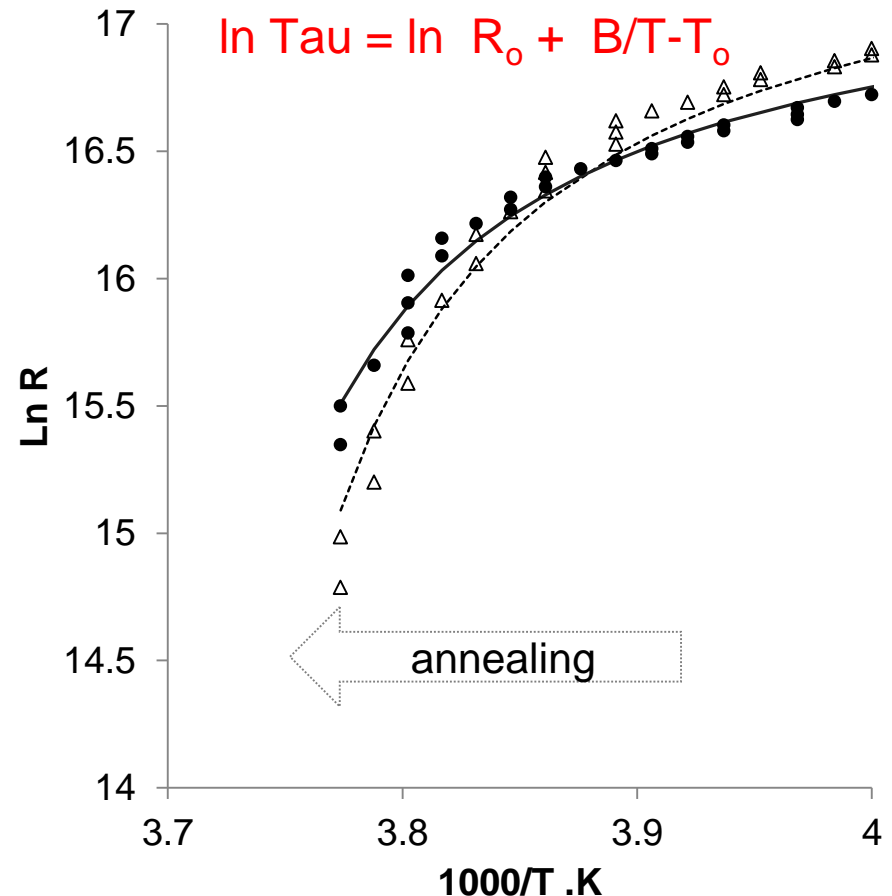


No.	Glass-forming material
1.	SiO <sub>2</sub>
2.	GeO <sub>2</sub>
3.	K <sub>2</sub> O·3SiO <sub>2</sub>
4.	Li <sub>2</sub> O·2B <sub>2</sub> O <sub>3</sub>
5.	SrO·2B <sub>2</sub> O <sub>3</sub>
6.	As <sub>2</sub> Se <sub>3</sub>
7.	GeS <sub>2</sub>
8.	Se
9.	Zr <sub>46.75</sub> Ti <sub>8.25</sub> Cu <sub>7.5</sub> Ni <sub>10</sub> Be <sub>27.5</sub>
10.	Pd <sub>48</sub> Ni <sub>32</sub> P <sub>20</sub>
11.	Pd <sub>77</sub> Cu <sub>6.5</sub> Si <sub>16.5</sub>
12.	Au <sub>76.9</sub> Ge <sub>13.65</sub> Si <sub>9.45</sub>
13.	50ZrF <sub>4</sub> -40BaF <sub>2</sub> -2NaF-8AlF <sub>3</sub>
14.	[Ca(NO <sub>3</sub> ) <sub>2</sub> ] <sub>0.4</sub> [RbNO <sub>3</sub> ] <sub>0.6</sub> (CRN)
15.	Sorbitol
16.	Xylitol
17.	Tripropylene glycol (TPG)
18.	Dipropylene glycol (DPG)
19.	Propylene Glycol (PPO-4000)
20.	1:8 NaCF <sub>3</sub> SO <sub>3</sub> -PPO(4000)

Physics Procedia 48 (2013) 113-119

## VTF Fit to describe the above $T_g$ resistance

- Above  $T_g$  the temperature dependence of the product resistance follows the Vogel-Tammann-Fulcher function.
- The curvature of the resistance plot decreases following annealing which relates to the increased strength of the glassy material.

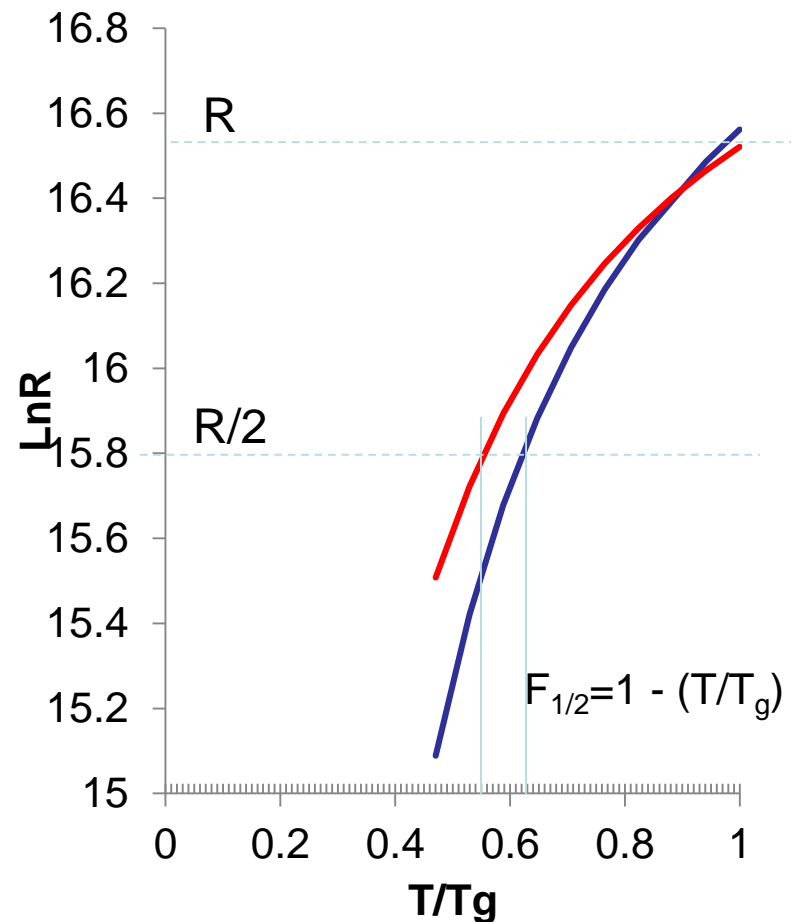


# Annealing impact on glassy matrix

- The fragility is a dimensionless parameter employed to explain the strength of a glassy material, it is calculate from

$$F_{1/2}=1 - (T/T_g)$$

- Fragility index range from 0-1 in the increasing order of strength.
- The fragility (or the steepness index) of the glassy material increase from 0.38 to 0.44 after annealing.
- Link b/w fragility and (i) moisture content of the unfrozen phase ?, (ii) ease of moisture desorption during 2 drying ??

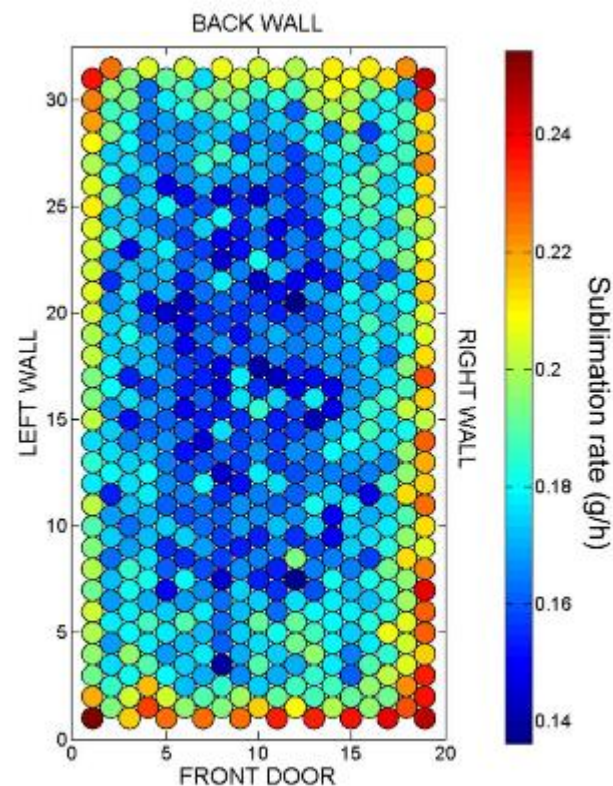


# Macroscale 2 Clusters of vials

- Steady state sublimation rate can vary by up to 50% across the shelf

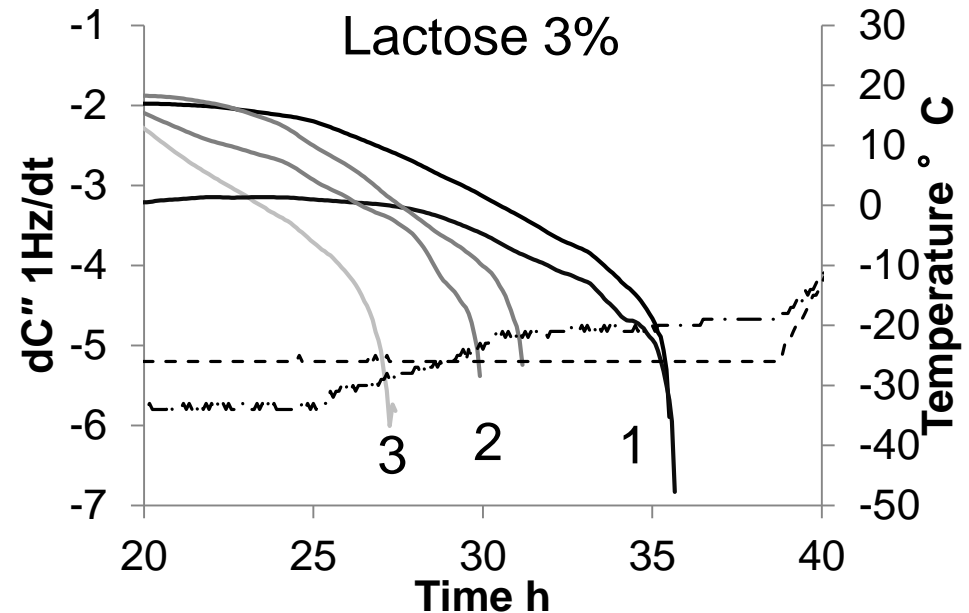
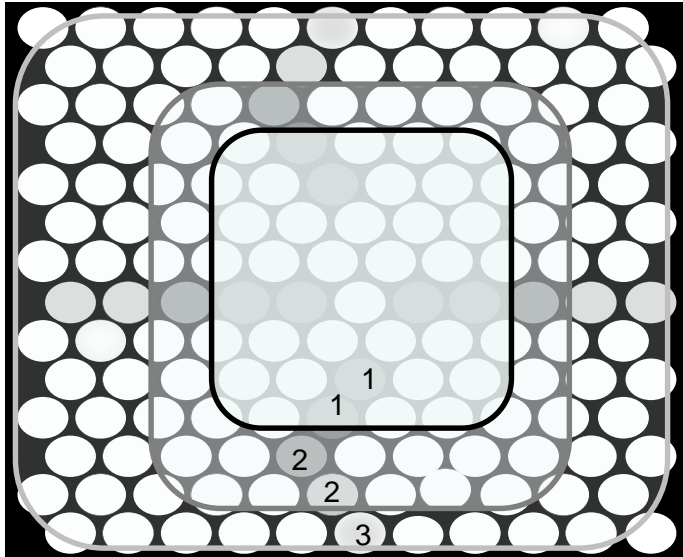
## Mini-piloting

- Mini-pilot studies should aim to capture the impact of the radiant heating.
- Aim: determine the minimum cluster size across which both core and edge processing effects can be determined
- Screen formulations for low impact from to edge effects (radiant heating)



Kauppinen, A. (2015) 26<sup>th</sup> Ann. Symp. Finnish Soc. Phys. Pharm., Kuopio, Finland

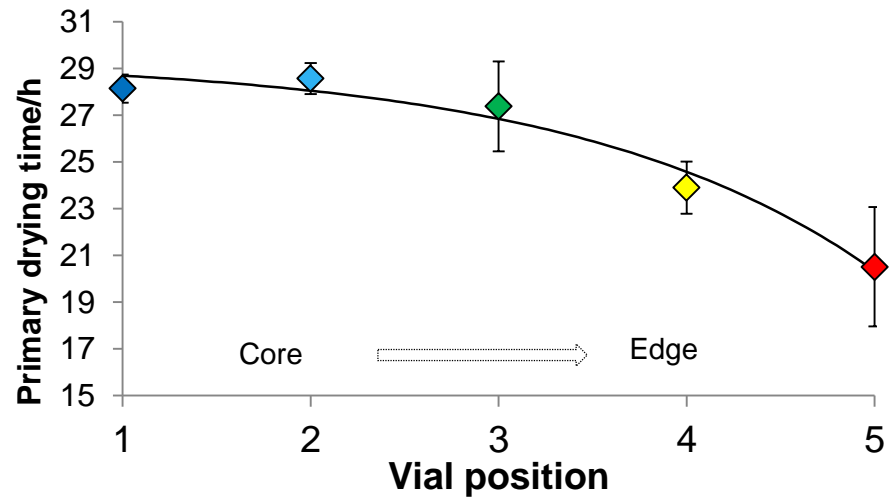
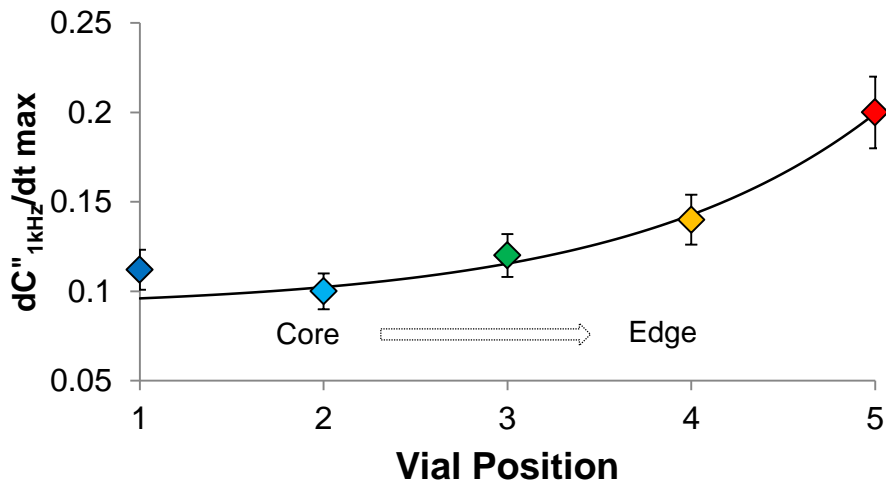
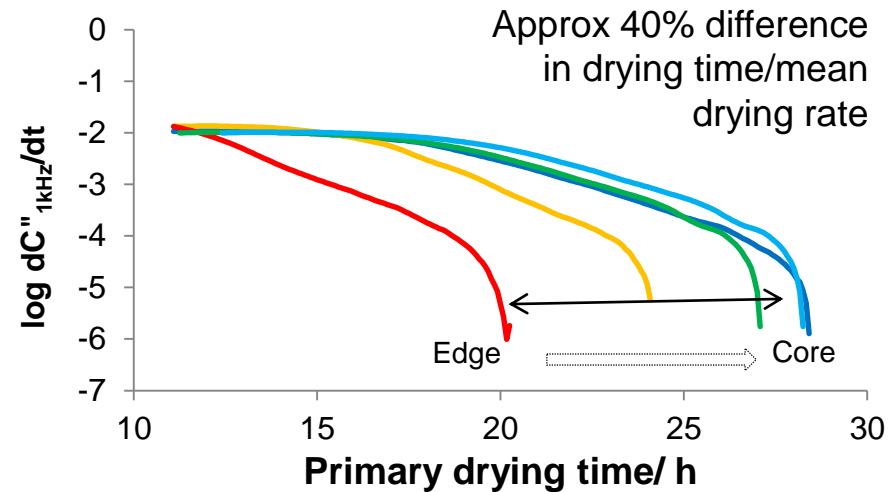
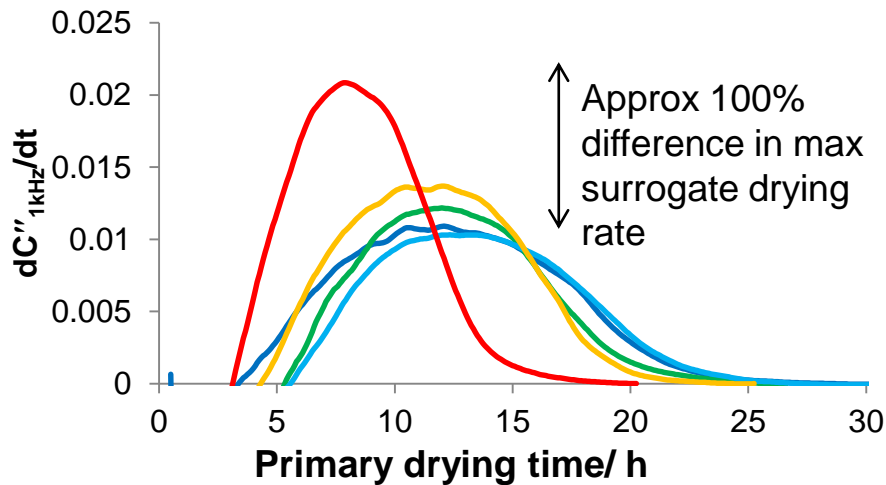
# Spatial mapping: Primary drying times



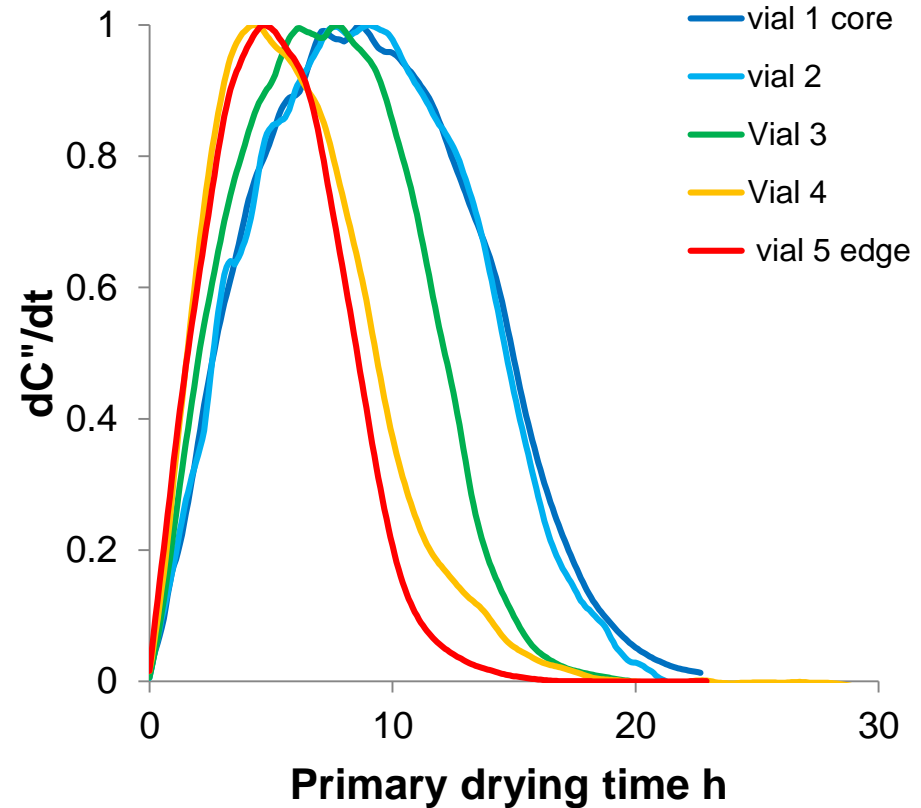
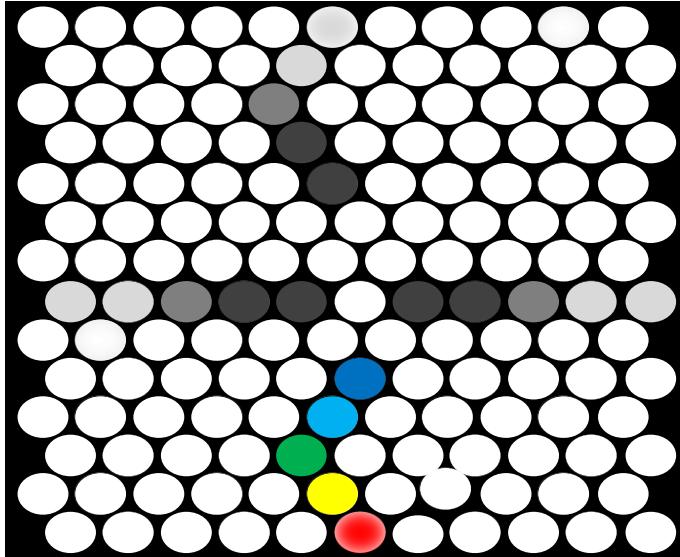
1. Primary drying time distribution across the shelf identifies three distinct spatial regions characteristic of thermal variations in the shelf.
2. Edge effects – may extend across three vials around the periphery of the shelf



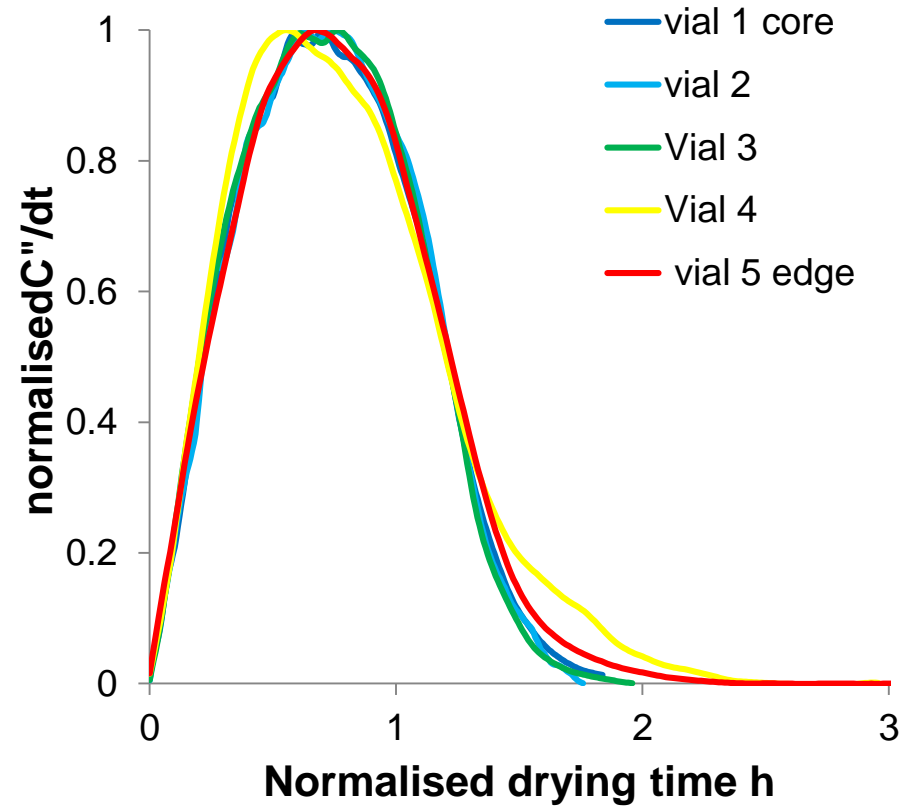
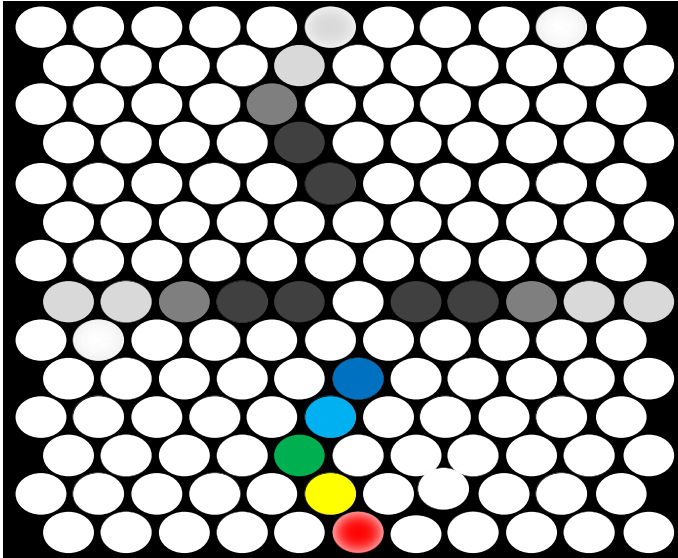
# Drying times & surrogate drying rates



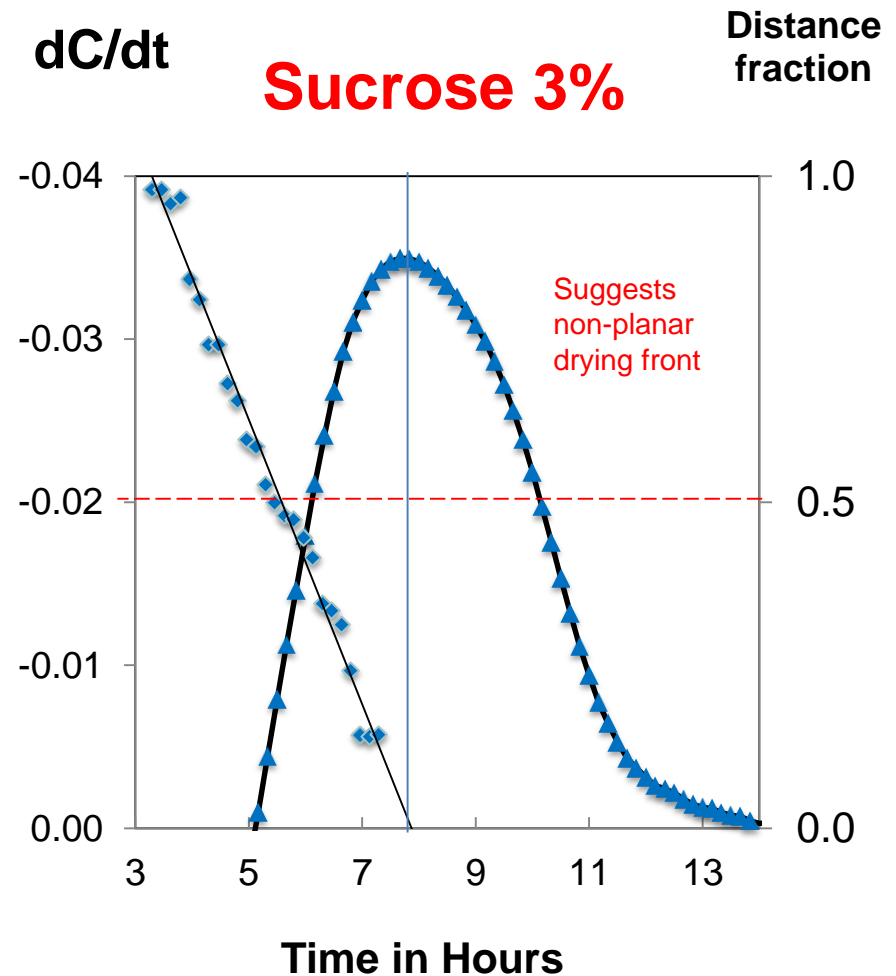
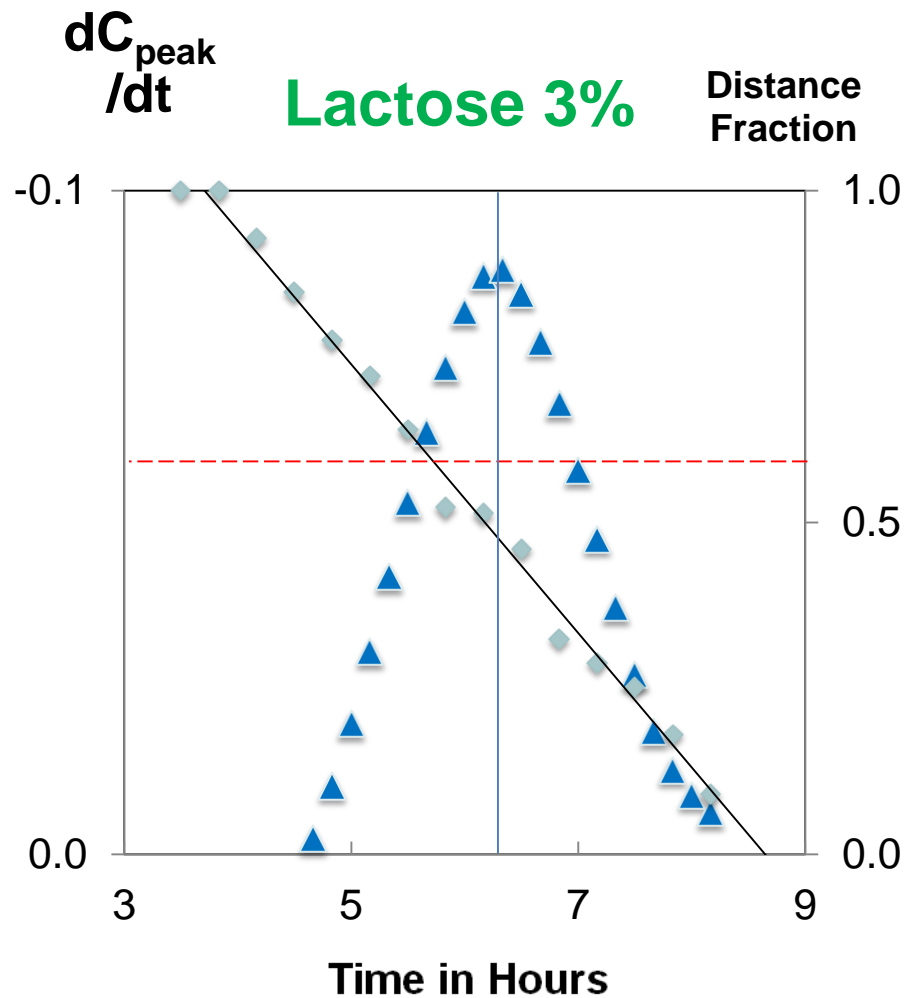
# Normalised Drying Curves – surrogate rates



# Normalised Drying Curves – drying times



# Shape of the drying front ?

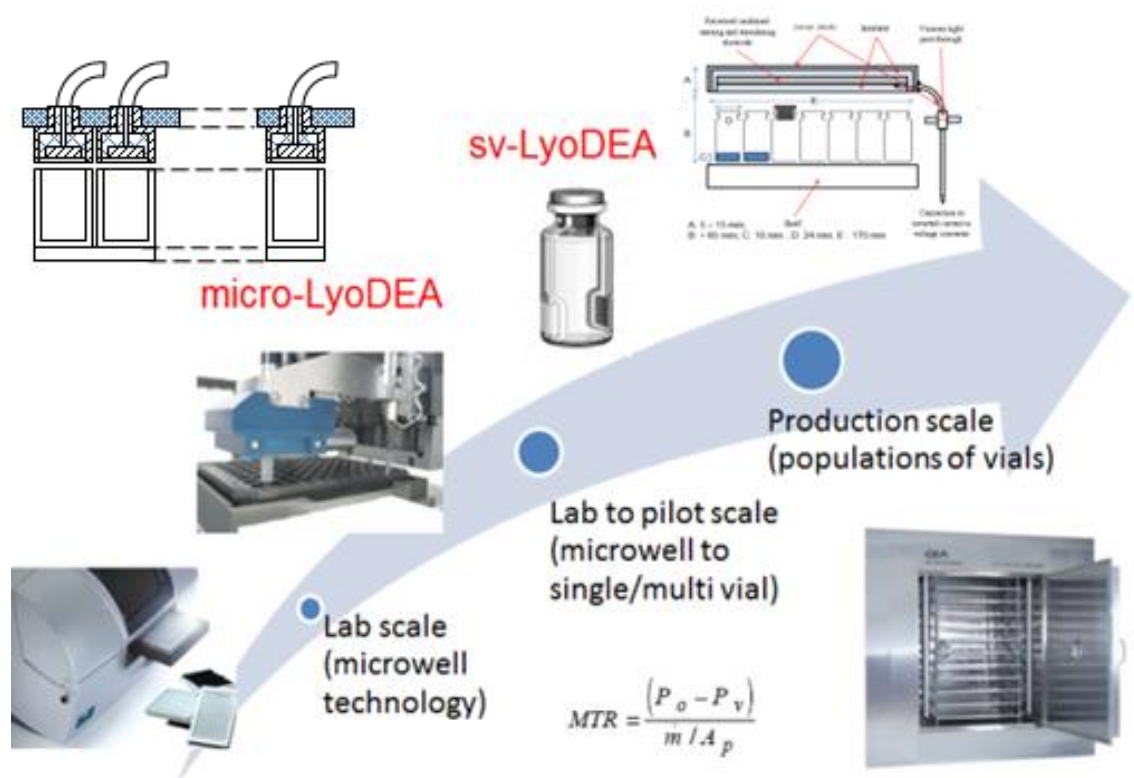


## Collaborative R&D project

- GEA Pharma Systems, BlueFrog,
- National Institute for Biological Standards and Control,
- Genzyme Ireland,
- De Montfort University

3 year project to implement TVIS across different scales:

- microtitre plates up to pilot scale



Supported by UK government

**Innovate UK**



# Opportunities and Challenges

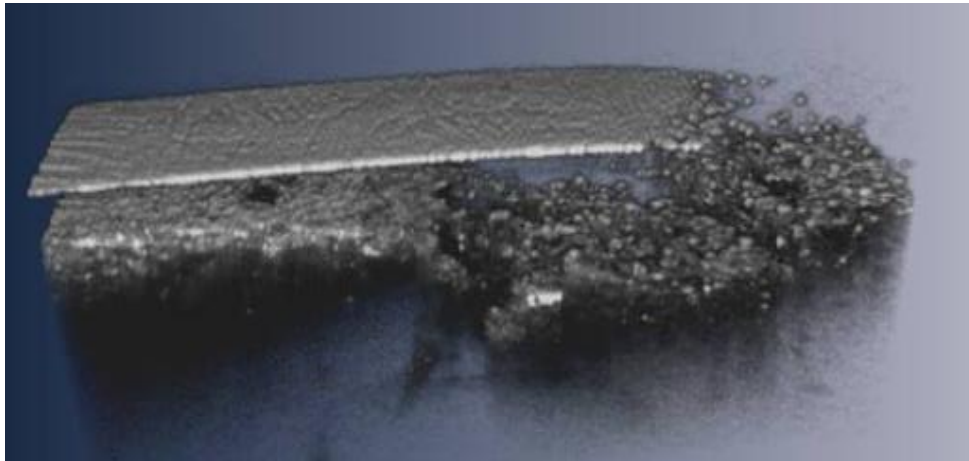
- TVIS registers thermal events through changes in the sample resistance associated with the exo thermic processes of ice formation and eutectic formation
- TVIS registers the glass transition through a discontinuity in either the capacitance or resistance as a function of temperature/time
- Primary drying (loss of ice) is monitored through changes in the strength of the dielectric loss peak (or step in the real part capacitance) – requires calibration (e.g. microbalance)
- Temperature control might be possible through monitoring of  $\log f_{\text{peak}}$  – requires calibration with external TCs
- Mechanisms of annealing where elucidated from changes in resistance with time (during the heating-hold phase) and from the absence of any changes in  $T_G$
- Drying rate profiles may provide information on the shape of the drying front and the influence of formulation on the susceptibility to radiant heating.
- Meso-structural information was extracted through the (non-Arrhenius) temperature dependence of the resistance
- Opportunities to track the physical characteristics of collections of vials is proposed.

# Acknowledgements

- **Evgeny Polygalov**. Senior Research Fellow. Leicester School of Pharmacy. De Montfort University
- **Dr Sohail Arshad**. Assistant Professor Pharmaceutics, Faculty of Pharmacy, Bahauddin Zakariya University, Multan, Pakistan
- **Dr Irina Ermolina**. Senior Lecturer. Leicester School of Pharmacy. De Montfort University
- **Julian Taylor and Trevor Page**. GEA Pharma Systems, Eastleigh, United Kingdom
- **Tim McCoy** Genzyme
- **Paul Matejtschuk** NIBSC
- Technology Strategy Board and Innovate UK

# Collapse in situ imaging of collapse

- **Optical coherence tomography-based freeze-drying microscopy provides in situ assessment of the collapse temperature**
- $T_C$  can be a few degrees different to  $T_C$  measured by conventional FDM
- Possible consequence of the differences in  $T_G$  prime that results from the freezing process impacting the amount of ice that forms.



Mujat et al. (2012) Biomedical Optics Express **3** 55-63